國立交通大學

機械工程學系

碩士論文

自行車自動變速策略之研究

Development of an Automatic Bicycle Shifting Strategy

Based on Human Factors Modeling

研究生：蔡岳良

指導教授：洪景華

共同指導教授：林聰穎

中華民國九十六年六月

自行車自動變速策略之研究

Development of an Automatic Bicycle Shifting Strategy Based on Human Factors Modeling

研 究 生：蔡岳良　　Student: Yueh-Liang Tsai
指導教授：洪景華 林聰穎　　Advisor: Chinghua Hung, Tsung-Yin Lin

國 立 交 通 大 學

機 械 工 程 學 系

碩 士 論 文

A Thesis
Submitted to Department of Mechanical Engineering
College of Engineering
National Chiao Tung University
in Partial Fulfillment of the Requirements
for the Degree of
Master
in
Mechanical Engineering

June 2007

Hsinchu, Taiwan, Republic of China

中華民國九十六年六月

自行車自動變速策略之研究

研究生：蔡岳良　　指導教授：洪景華 林聰穎

國立交通大學機械工程學系

摘要

自行車騎乘者因為各種因素的考量，有時需要高效率，但有時需要較低的踩踏力以避免受傷，因此騎乘者可依據各種需要而調整變速撥桿，選擇不同檔位以獲得符合需求的最佳踏速，而現今的研究文獻也分別指出符合不同單一需求下，如較低的肌肉應力或較低的關節扭矩考量下的最佳踏速範圍，但是如此一來便會忽略了其他因素；另外由於大多數騎乘者的經驗不足，不能充分的發揮變速系統的效用，或是會選擇不適當的檔位，除了浪費力氣以外，更可能在不自覺中受傷。

本研究將使用模糊理論整合自行車踩踏時的各種因素，依據不同的需求和騎乘環境決定出上下檔位的時機，如此便可提供一完整的變速策略，為了能使該變速策略和變速系統能有效被充分的利用，故配合文獻中的換檔路徑方式完成一自動變速系統策略之設定，最後利用 Browning SmartShift 之系統將本文所發展之策略具體化，並配合實際道路測試，確認系統反應符合騎乘者之需求。

Development of an Optimum Bicycle Shifting Strategy

Based on Human Factors Modeling

Student: Yueh-Liang Tsai Advisors: Chinghua Hung, Tsung-Yin Lin

Department of Mechanical Engineering

National Chiao Tung University

ABSTRACT

During cycling, riders can move shift-levers to obtain different gear-ratio or cadence in order to satisfy different external environments and cardiovascular requirements such as high power, low pedaling force, low muscle stress, and etc. Prior researches of human cycling focus on satisfying the specific one or two requirements to determine the optimal cadences. But most inexperienced riders can not judge the moment to shift gears to obtain the optimal cadence. Such actions will injure rider's body, and riders can not make use of the derailleur system in the correct way.

This study used fuzzy control theory to integrate all requirements in cycling and developed the strategy about the correct up-shifting or down-shifting moment depending on all cardiovascular requirements and external physical environments. Finally, this study proposed a more complete strategy to certify rider's health. On the hand, this study combined the gear-shifting sequence from prior researches to use all gear-ratios during cycling. Finally, Browning SmartShift system is used to implement the proposed method. Road tests were also performed to ensure the system reactions do meet users' requirements.

ACKNOWLEDGEMENT

兩年的時間雖然不長，但是卻發現自己受到了好多的照顧，最感謝的就是 曾錦煥老師，從大三的暑假跟著老師做專題，以及到後來順利推甄進入研究所學習，也在老師的不嫌棄之下進入了應用最佳化實驗室，大四下學期接受老師的指導與照顧，如果學生能夠跟同儕有那麼一點不一樣，都是因為老師的提點與關懷，認識老師的時間才短短的一年多，卻從老師的身上學習到許多，無論是身教或是言教，老師的人生智慧和學術涵養都讓學生受益良多，然而這段時間最讓學生懷念的，就是老師您的身影。

感謝 蔡忠杓老師和 洪景華老師，在我們失去曾老師，最無助和最徬徨的時候，伸出援手照顧我們，這段時間給了學生最大的幫忙以及心理的支撐，特別感謝 林聰穎老師指導學生的論文，不吝惜的教導學生並且樂於解決學生的問題，還會帶著學生出外散心消除壓力，感謝這三位老師的耐心以及關愛，承蒙老師們照顧我這不成材的學生了。

感謝口試委員： 徐瑞坤老師和 呂東武老師的指導，給予學生許多意見並且讓學生的論文能夠更加的完整，感謝老師們的耐心指教以及用心付出。

感謝實驗室的學長姐們，總是願意花費自己的時間幫助學弟，無論是論文的問題、生活的問題、感情的問題，學弟總是能感受到學長姐的關懷，在曾老師離去之後，學弟最常接觸的就是你們，這段時間受惠良多，學弟對於能夠認識這麼一群學長姐感到無限的感激。感謝實驗室的同學，能和我一起在學業上努力和處理實驗室的大小雜事，雖然對彼此的題目不熟悉，但是卻時常能給予我跳脫性的想法和意見，兩年來扶持著我，讓我成長和學習，也從你們身上看到了許多我沒有的優點，這是我加入應用最佳化實驗室最美好的收穫。

感謝我的大學同學們，雖然大家在不同的研究室奮鬥，但是卻始終能夠維持感情、互相幫忙，我會很懷念在交大的這段時間，希望大家以後都能飛黃騰達，一切平安

最後要感謝我的家人，這段時間以來的全力支持，讓我能夠心無旁騖的在學業上衝刺，如果沒有你們，我也沒有辦法完成這本論文，謝謝你們的照顧和包容。

TABLE OF CONTENTS

LIST OF TABLES

LIST OF FIGURES

NOTATIONS

v	velocity
u	pedaling cadence
g	gear-ratio
$\mu_V(v)$	membership function of velocty
$\mu_U(u)$	membership funtion of pedaling cadence
$\mu_G(g)$	membership function of gear-ratio

CHAPTER 1

INTRODUCTION

1.1 Bicycle Derailleur System

In 1886, John Kemp Sterley and William Sutton invented the first bicycles. About one hundred years later, bicycle design technologies were developed very well in order to ride more comfortable and efficient. In recent years, multi-speed bicycle has become the market stream. A multi-speed bicycle is composed of lots of components, including frame tubes, brakes, derailleur systems and transmission parts. A complete derailleur system, as shown in Fig 1.1 and Fig 1.2, consists of five components: chainwheel and freewheel, front and rear derailleurs, shift levers, cables and a chain. The chainwheel and freewheel include several chainrings and cogs, each having different numbers of teeth. There are two shift levers connected to the front and rear derailleurs through cables. Cyclists move the two shift levers to drive derailleurs guiding the chain to engage larger chainrings, or guiding the chain to drop to smaller chainrings. It can get different gear-ratios for cyclist.

When riding a bicycle, the cyclist makes significant use of both the strength in legs and the cardiovascular system. Change gear-ratios can make riders feel more comfortable. Cyclists can choose a low gear-ratio to pedal at high cadence and low torque, or choose a high gear-ratio to pedal at low cadence and high torque. It has many factors to decide which gear-ratio to be selected. The optimal gear-ratio can get the optimal cadence. Cyclists will feel comfortable if they pedal at their optimal cadence. When external physical environment changes, cyclists can change the gear-ratio to get their optimal cadences. It is important to decide what the optimal cadence is, and how to choose an optimal cadence when external physical environment changes.

Fig 1.1 Bicycle derailleur system [1]

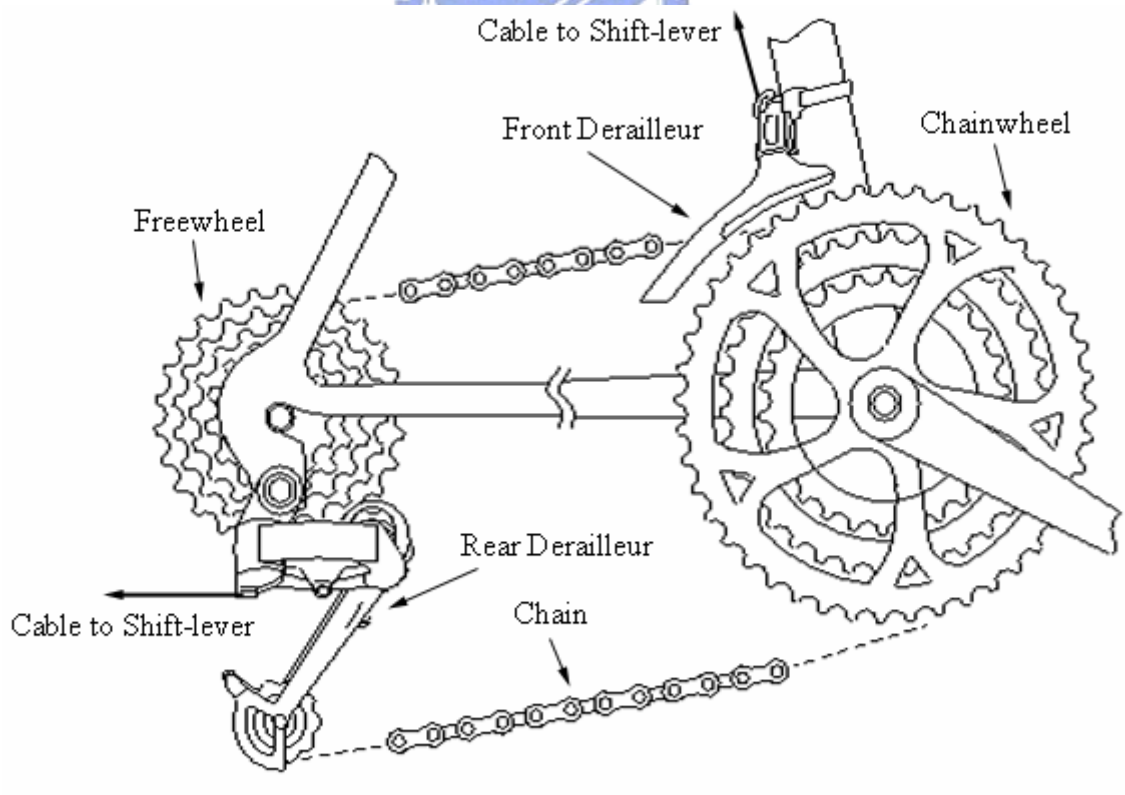

Fig 1.2 A detail bicycle derailleur system [1]

1.2 Motivation

In recent years, there are more and more people riding bicycles for recreation. People hope to ride bicycle more comfortable and with better performance. What they need is to know the selection of the optimal cadence and ride bicycle at the optimal cadence. There are lots of factors which influence how to choose the optimal cadence. For example, muscle stress, joint moment, human power, torque, and etc. In the past, many researches focused on one or two factors to determine the optimal cadence. From these researches, riders can get some rules to help them riding bicycle at the optimal cadence. But riders still feel uncomfortable because there are some factors neglected. For example, riders can choose the optimal cadence between 50 and 60 rpm from the ergonomic point of view, but such cadence may make knees easy to get injury in biomechanics.

There are such researches about the time to change gear-ratio to get the optimal cadence when the external physical environment has been changed. Also, an inexperienced rider can not judge the moment to use the shift-levels to get the optimal cadence. So they can not make use of the derailleur system in a correct way.

However, there are no researches about choosing the optimal cadence by considering all factors mentioned above. But on the market, there are some products which can change gears automatically such as Browning SmartShift and Shimano AutoD. But the gear changing criteria of these products only depends on the bicycle velocity. In facts, it is not enough for humans.

According to the above statements, the purpose of this research is to develop a model considering all factors affecting the human optimal cadence. In addition, this study also provides rules about how to choose a correct gear-ratio as the external physical environment changes. Finally, the system can change gears automatically so that anyone can ride bicycle easily and make full use of the derailleur system.

1.3 Literature Review

In order to ride at the optimal cadence, there are lots of researches defining optimal cadence from different standpoints. In 1986, Rob Redfield and M. L. Hull developed a biomechanical model to compute stress and moment when riding bicycles. They found the relation between joint moments and pedaling rates with experiments. They tried to minimize the sum of the average absolute joint moments during constant power riding. They found the optimal cadence was about 95 to 105 rpm [2], and experimented for lowering muscle stress or joint moment. From the experiment, they got the high connection between muscle stress and other factors (such pedal force, and ankle moment) [3]. In 1988, M. L. Hull and his coworkers chose to lower muscle stress. And they developed a more sophisticated model to assess the influence of cadence on the muscle stress. They minimized the muscle stress and got the optimal cadence about 95 to100 rpm [4].

In 2000, Anthony P. Marsh [5] and his coworkers made an experiment. They divided three groups of cyclists: trained cyclists, runners and less-trained cyclists. These cyclists experimented at optimum cadence and optimum output powers. The trained cyclists and runners rode at 100 W, 150 W, 200 W, and 250 W; the less-trained cyclists rode at 100 W and 150 W. A simulation and analysis about the specific neuromuscular activation, force, stress and endurance based on a dynamic model carried out at different rates of 75, 90 and 105 rpm at a fixed power output of 265 W [6]. An optimum power output of the amateur cyclist is about 75 W [7].

One experiment measured the preferred cadence and the lowest oxygen consumption cadence. Eight cyclists and eight non-cyclists pedaled at 200 W. The preferred cadence for cyclists is 75 to 95 rpm. But the lowest oxygen consumption cadence for cyclists is 50 to 60 rpm [8]. From these researches, it is important to consider all factors influencing the optimal cadence. Because it has a obvious difference from different points of view.

1.4 Thesis Outlines

In order to develop a model including all factors affecting the optimal cadence, the cycling model and factor analysis have be done in this thesis. And the model can help to determine how to choose a suitable gear ratio. The brief description of outlines on this thesis contents are given as follows.

Chapter 2 is the preliminary details which include brief introduction about lower limb in anatomy and some terminology on the bicycle. Chapter 3 introduces that the factors influence human cycling and the effect of this factors about rider's performance. Chapter 4 proposes the basic concept and detail design steps for fuzzy logic controller. And the fuzzy logic controller of the gear-shifting is designed in Chapter 4. In Chapter 5, this study constructs the experiments machines by combing the software and hardware. And it has discussion about test results and compare to the Browning SmartShift system. Finally, Chapter 6 contains the conclusions and future works, which could assist some aspects for following works on this study.

CHAPTER 2

PRELIMINARY DETAILS

2.1 Lower limb in Anatomy

Human beings use their lower limb to ride a bicycle. But lower limb have complex constructions. In order to make it easy understanding, its structure can be divided into three groups. This section will introduce the lower limb constructions by the anatomy point of view.

2.1.1 Bones

The lower limb carries the entire weight of the stand body, and is subjected to exceptional forces when people jump or run. Thus, it is not surprising that the bones of the lower limbs are thicker and stronger than the comparable bones of the upper limbs. The three segments of the free lower limb are the thigh, the leg, and the foot. As shown in Fig 2.1, the main bone of the thigh is femur. The head of the femur is the ball that articulates with the acetabulum. This head is mounted on a neck, a projection from the femur. Two ridges extend from the femur for the attachment of muscles. The main bones of the leg are tibia and fibula. The distal region of the leg is supported by the tibia and fibula. The tibia is the larger of these two; it directly articulates with the femur. The fibula articulates the tibia at its proximal end. The main bones of the foot are tarsal, metatarsals and phalanges. The tarsal bones directly articulate with tibia and fibula. Metatarsals extend the length of the foot. The toes contain phalanges, just as the fingers do.

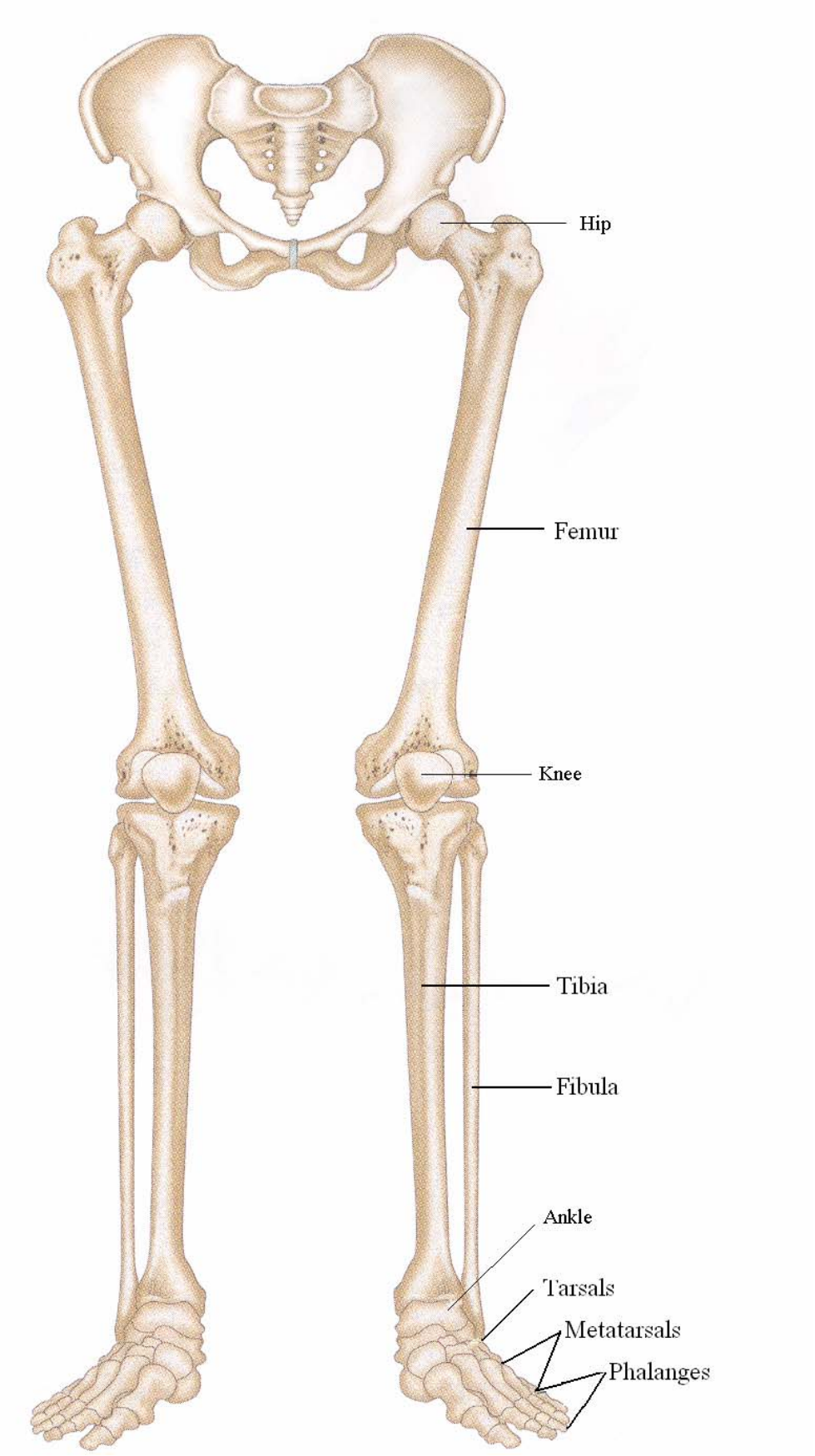

Fig 2.1 The bones of lower limb [9]

2.1.2 Muscles

There are lots of muscles at the lower limb. Introducing these muscles from hip to ankle can make it easy to understand. There are two directional terms: anterior and posterior. Anterior means toward the front of the body, and posterior means toward the back of the body. The anterior muscles that move the thigh at the hip all function to flex and laterally rotate the hip. The posterior muscles extend, abduct, and some medially rotate the hip. That detail information are showed in Table 2.1. The medial muscles that move the thigh at the hip have all functions to adduct the thigh, as shown in Table 2.2.

Table 2.1 The muscles that move the thigh at the hip [10]

		Origin	Insertion
Muscle	Iliacus	iliac fossa	lesser trochanter of femur
	Psoas major	transverse process of lumbar vertebrae	lesser trochanter of femur
	Gluteus maximus	iliac crest, sacrum, coccyx, aponeurosis of lumbar region	gluteal tuberosity and iliotibial tract
	Gluteus medius	lateral surface of ilium	greater trochanter of femur
	Gluteus minimus	lateral surface of ilium	greater trochanter of femur
	tensor fasciae latae	anterior border of ilium and iliac crest	iliotibial tract

Table 2.2 The medial muscles that move the thigh at the hip[10]

		Origin	Insertion
Muscle	Gracilis	symphysis pubis	proximomedial surface of tibia
	Pectineus	pectineal line of pubis	distal to lesser trochanter of femur
	Adductor longus	pubis	linea aspera
	Adductor brevis	pubis	linea aspera
	Adductor magnus	inferior rami of pubis and ischium	linea aspera and medial epicondyle of femur

The muscles of the thigh that move the leg are divided into an anterior group and a posterior group. The primarily function of the anterior group is to extend the leg at the knee, and the function of the posterior group is to extend the thigh at the hip and flex the leg at the knee, as shown in Table 2.3.

Table 2.3 The muscles of the thigh that move the leg [10]

		Origin	Insertion
Muscle	Sartorius	anterior superior iliac spine	medial surface of tibia
	Rectus femoris	anterior superior iliac spine	patella by common tendon
	Vastus lateralis	greater trochanter and linea aspera	patella by common tendon
	Vastus medialis	medial surface and linea aspera	patella by common tendon
	Vastus intermedius	anterior and lateral surfaces of femur	patella by common tendon
	Biceps femoris	ischial tuberosity; linea aspera	head of fibula and lateral epicondyle tibia
	Semitendinosus	ischial tuberosity	proximal portion of shaft of tibia
	Semimemebranosus	ischial tuberosity	medial epicondyle of tibia

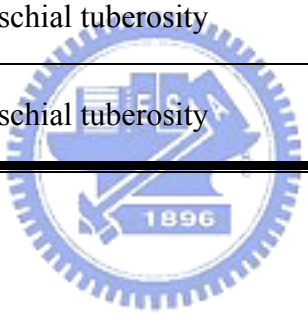

The muscles of the leg that move the ankle, foot, and toes are separated into an anterior group (including tibialis anterior) that dorsiflexes the foot and extends the digits, a lateral group (the peroneal muscles) that aid in dorsiflexion and eversion, and a posterior group (including gastrocnemius and soleus) that plantar flexes the foot and flexes the toes. The descriptions are shown in Table 2.4.

Table 2.4 The muscles of the leg that move the ankle [10]

		Origin	Insertion
Muscle	Tibialis anterior	lateral condyle of tibia	1st metatarsal and tarsal
	Gastrocneumius	lateral and medial epicondyle of femur	posterior surface of calcaneus
	Soleus	posterior aspect of fibula and tibia	calcaneus

Several muscles shown in Fig 2.2 and 2.3, are the main power source when riding bicycles. Rectus femoris is the superficical muscle of the anterior thigh and the longest head, and it is the only muscle in the group crossing the hip point. It runs straight down the thigh. The Vastus lateralis forms lateral aspect of the thigh. It is a common intramuscular injection site, particularly in infants. Vastus medialis forms inferomedial aspect of thigh. Vastus intermedius is obscured by rectus femoris. It lies between vastus lateralis and vastus medialis on the anterior thigh. Gluteus maximus is the largest and most superficial of gluteus muscles. It forms bulk of the buttock mass. Its fibers are thick and coarse. It overlies the large sciatic nerve and covers the ischial tuberosity only when standing. When sitting, it moves superiorly leaving the ischial tuberosity exposed in the subcutaneous position. The Biceps femoris is lateral muscles of the posterior group and arises from two heads. The Tibialis anterior is superficial muscles of the anterior leg, and laterally paralles sharp anterior margin of the tibia. Gastrocnemius are superficial muscles of pair.

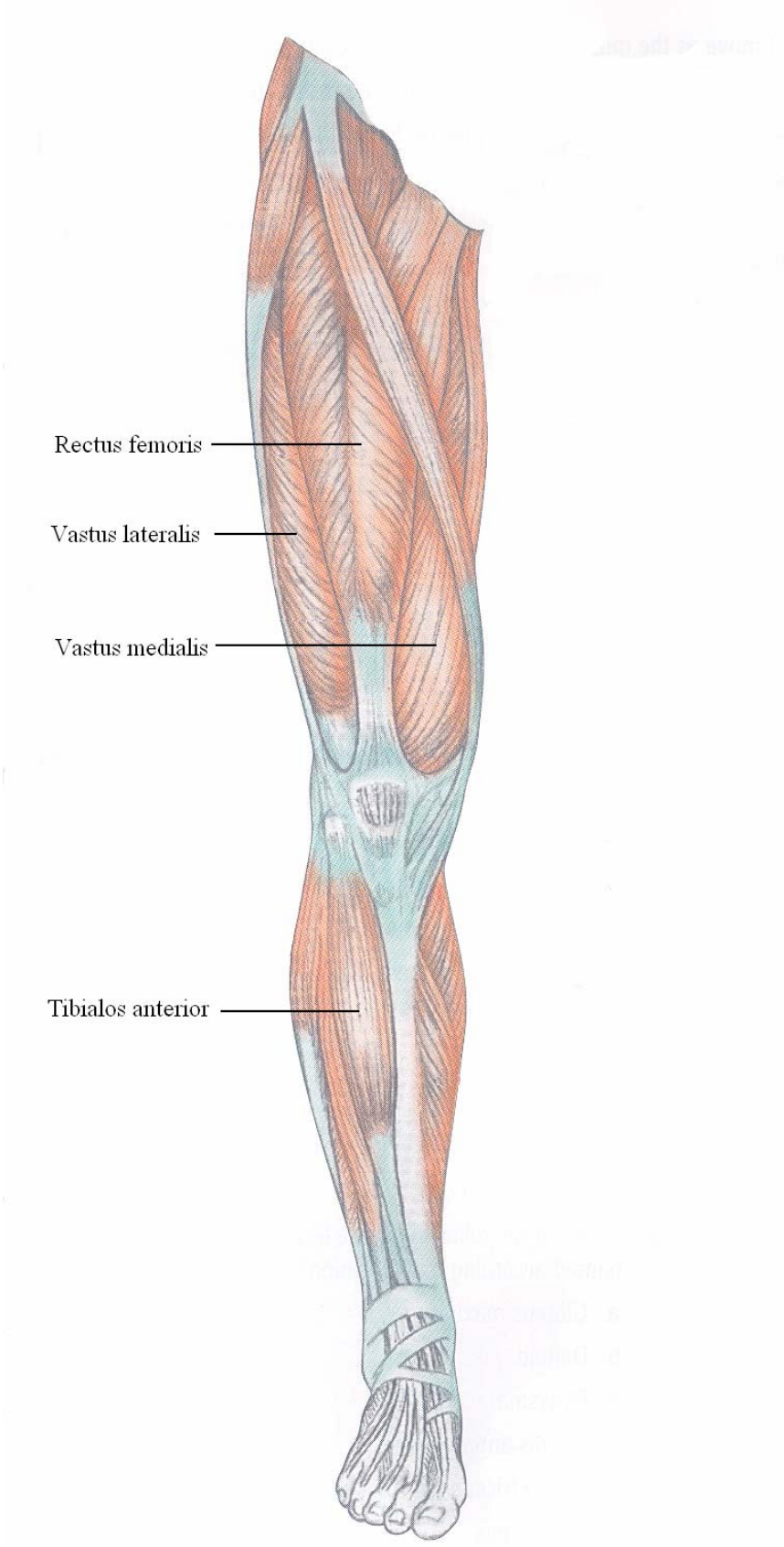

Fig 2.2 Lower limb muscles anterior [9]

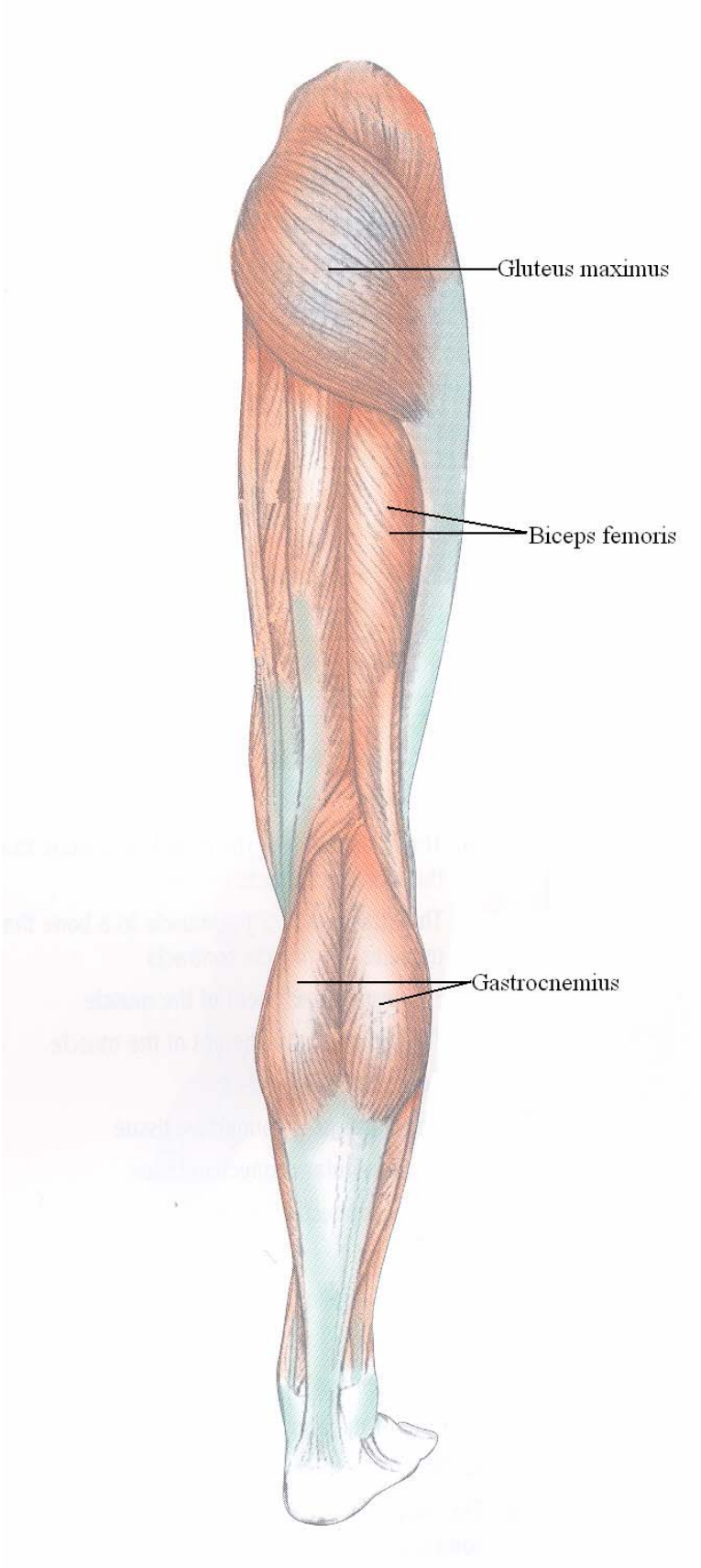

Fig 2.3 Lower limb muscles posterior [9]

2.1.3 Joints

There are three joints in the lower limb that is important during cycling. These three joints are hip joint, knee joint and ankle joint. All of these joints are synovial joints. The synovial joints are the most moveable joints of the body, and all are diarthroses. Each synovial joint contains a fluid filled joint cavity. Most joints of the body are synovial joints, especially those in the limbs. The hip joint articulates with coxal bone and femur. Its structural type is ball and socket of synovial joint. Its functions types are multiaxial, flexion, extension, abduction, adduction, rotation and circumduction. The knee joint includes tibiofemoral segment and femoropatellar segment. The structural types of these two segments are hinge of synovial joint and gliding of synovial joint. The function types of the tibiofemoral segment are uniaxial, flexion, extension and some rotation. The function type of the femoropatelar segment is gliding. The ankle joint articulates tibia and fibula with talus. Its structural type is hinge of the synovial joint. Its function type is uniaxial, flexion and extension.

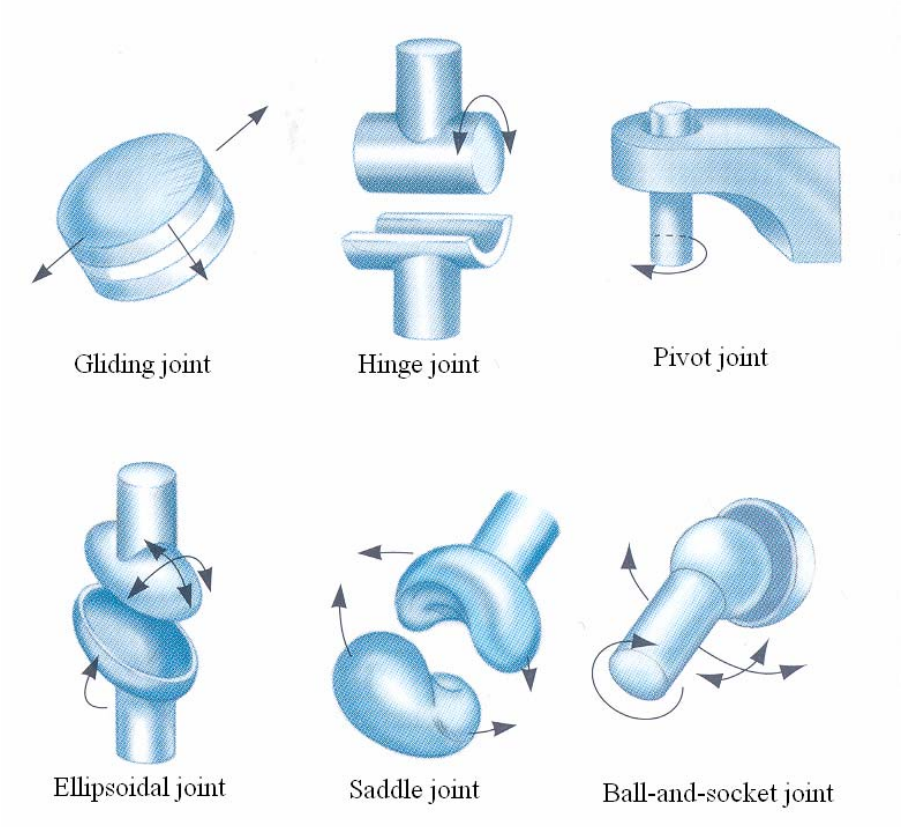

Fig 2.4 joint structure [9]

2.2 Definitions of terms

In this section, some concepts related to bicycle science will be presented. Some terminology used is introduced as follows:

1. Pedal forces:

   The feet generate forces acting on the pedals. The forces are usually between horizontal and vertical directions.

2. Muscle stress:

   Stress is used to describe the distribution of a force over the area on which it acts. It is expressed as force intensity, that is, forces per unit area.

$$Stress = \frac{Force}{Area} \tag{1}$$

   Muscle architecture is typically described in terms of muscle length, mass, myofiber length, pennation angle, and physiological cross-section area (PCSA). PCSA is an approximation of the total cross-section area of all muscle fibers, projected along the muscle's line of action. It is calculated as:

$$PCSA(mm^2) = \frac{M(g) \times \cos\theta}{\rho(g/mm^3) \times L_f(\text{mm})} \tag{2}$$

   where M is the muscle mass, ρ is the muscle density ($1.056\ g/cm^3$ in fresh tissue), θ is the surface pennation angle, and L_f is the myofiber length [11]. Therefore, use the pedal force divide by PCSA can obtain the muscle stress.

3. Joint moment:

   The moment of a force about a point is the vector product of the force and the distance:

$$M = r \times F = r \times F \times \sin\theta = F \times d \tag{3}$$

   where d represents the perpendicular distance from the point to the line of action of the force. Therefore, the moments from pedal forces act on hip, knee and ankle can be computed by the formula .

4. Human power:

   The capacity of a machine can be measured by the time rate at which it can do works or deliver energies. The power P developed by a force F which does an amount of work U is

   $$P = dU/dt = F * dr/dt = F * v \quad (4)$$

   Therefore, the power generated by human forces to make bicycle to go forward can be computed by this formula.

5. Torque:

   The component of the moment about the rotating axis of the subject is called the torque. The pedal forces act on the pedal and generate torques on the pedal axis.

6. Gear-ratio:

   It means front chainring teeth divided by rear chainring teeth.

7. Down-shifting:

   The chain is shifted from a larger chainring to a smaller chainring in the front derailleur system, or from a smaller chainring to a larger chainring in the rear derailleur. A smaller gear-ratio can be obtained.

8. Up-shifting:

   It is the reverse of down-shifting. A larger gear-ratio can be obtained.

9. EMG:

   The technique of recording the electrical activity produced by the muscle, or the myoelectric activity, is known as the electromyography (EMG). Electrodes placed on the skin surface and fine wires inserted into muscle are used to measure the voltage potentials produced by contracting muscles. The activity of the lower limb musculature is evaluated in this way with respect to the timing and the intensity of the contraction. Data collection of variables that affect the quality of the EMG signal include the placement of and distance between the recording electrodes, skin surface conditions, distance between electrode and target muscle, signal amplification and filtering, and the rate of data acquisition [11].

CHAPTER 3

CYCLING PERFORMANCE FOR HUMAN

3.1 Forces

Riders generate pedaling forces to make bicycles moving forward. If more forces are generated, the bicycles will go faster. At the same time, forces make people to generate joint moments and muscle stresses. These two factors make rider feel tired or even injure rider's body.

In 1985, M. L. Hull and M. Jorge measured normal and tangential pedal forces and joint moment [12]. They made a model to perform some detailed biomechanics analysis of the lower limb. In 1986, Rob Redfield and M. L. Hull made an experiment to test the relation between joint moments and pedaling rates at a constant power during cycling [2]. They used a five-bar linkage model to simulate the bicycle rider system as shown in Fig 3.1. They defined the optimal cadence which minimizes the sum of the average of the absolute hip and knee moments. As shown in Fig 3.2, they found that the cadence minimizes the hip moment of 12 N-m at 95 rpm and the knee moment of 17 N-m at 105 rpm. So they decided the optimal cadence is 90 to 105 rpm. They also made another experiment to minimize the two cost functions [3]. One is based on joint moments and the other is based on muscle stresses. Both cost functions offer reasonable predictions of pedal forces. But the muscle stresses cost function predicts better than joint moments as shown in Fig 3.3 and 3.4. Because the cost function of muscle stresses predicts hip moments that compare favorable with the actual hip moment.

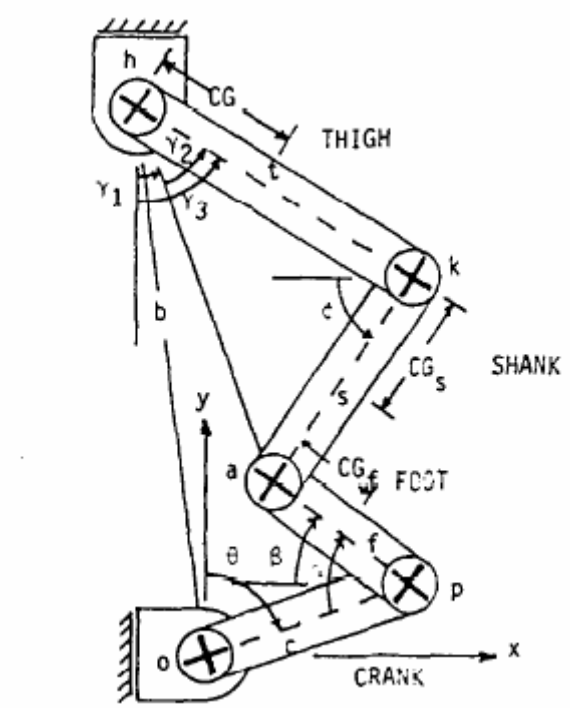

Fig 3.1 Five-bar linkage model [2]

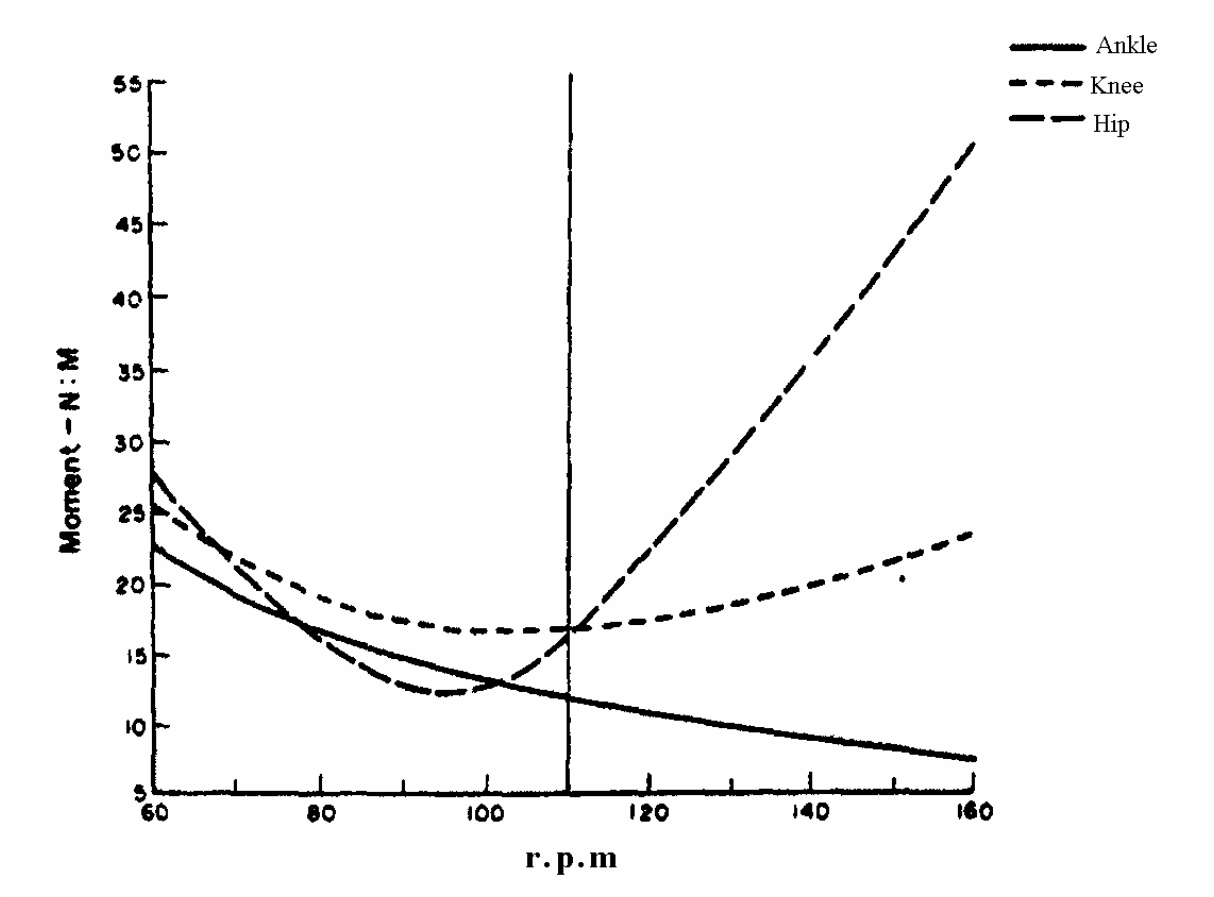

Fig 3.2 Average joint moments and cadence [2]

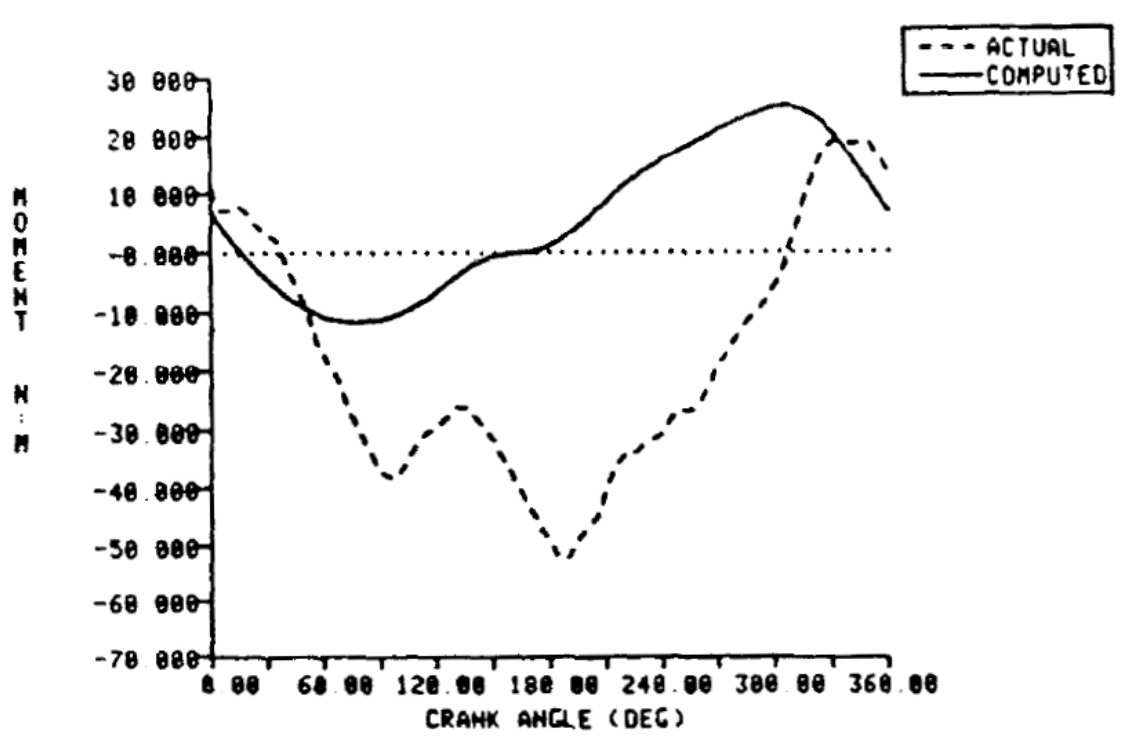

Fig 3.3 Hip moment comparison (moment case) [3]

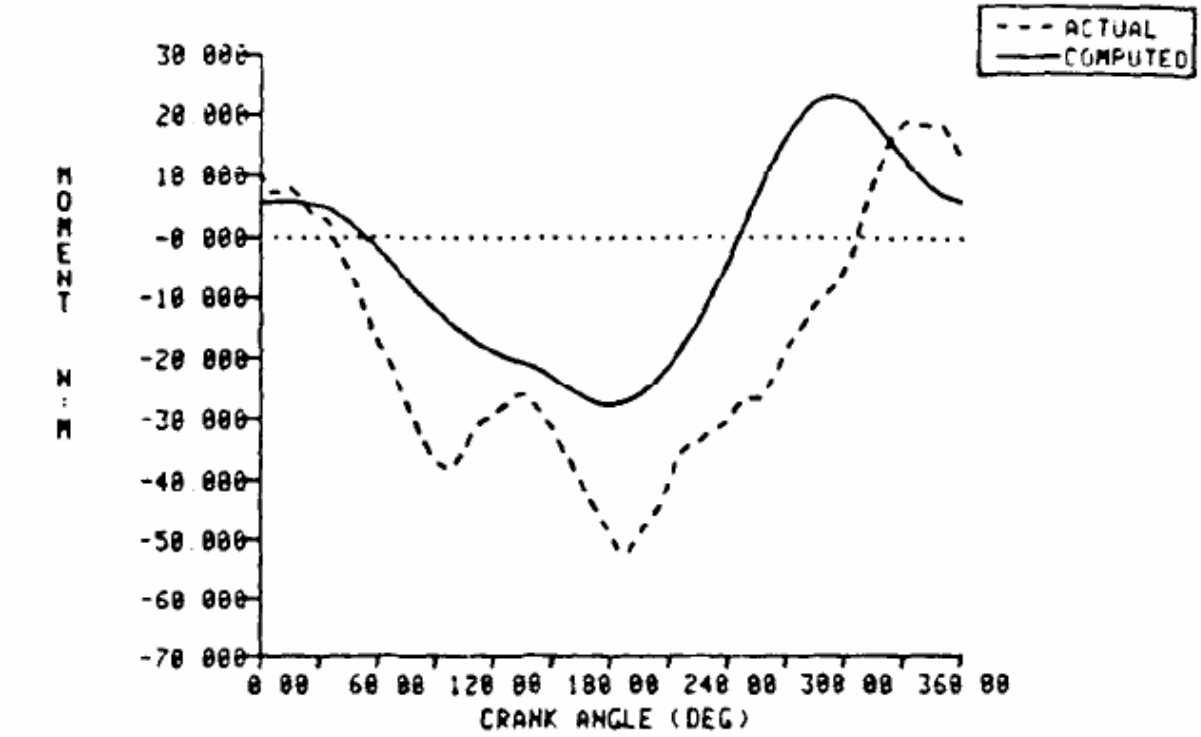

Fig 3.4 Hip moment comparison (stress case) [3]

In 1988, Hull, M. L. et al. [4] found the optimal pedaling rate using a muscle stress based objective function. They avoided redundant equations and computed stresses in 12 lower limb muscles. They also measured the stresses in muscles crossing the joint, but they thought it is less important than stresses in muscles at thigh and leg. As shown in Fig 3.5, the optimal pedaling rate falls in the range of 95 to 100 rpm. Its result agreed with the range founded by Rob and Hull in 1986 [4].

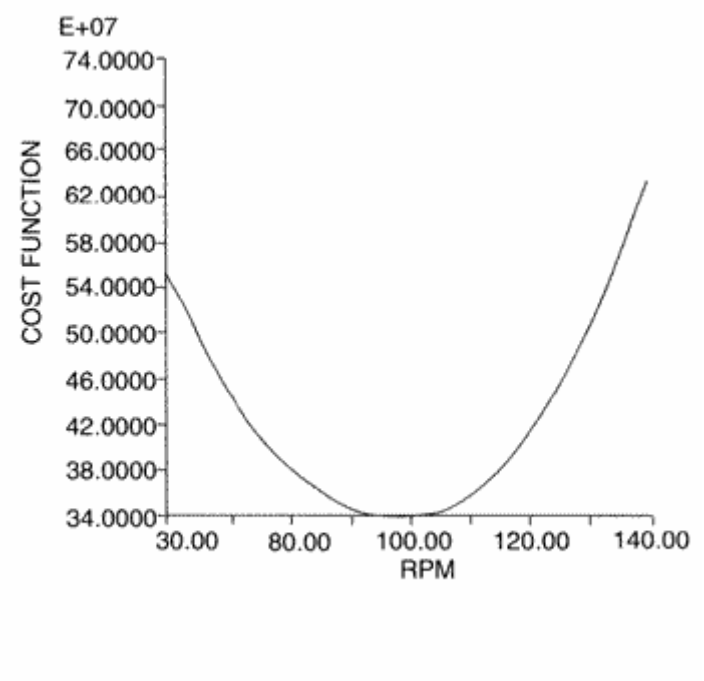

Fig 3.5 Muscle stress cost function [4]

In 1999, Neptune and Herzog [13] made experiments about pedaling forces and pedaling rates. As shown in Fig 3.6 the components of average resultant muscular and non-muscular pedaling force systematically decreased and increased respectively as pedaling rates increased. The total average resultant pedaling force varies with pedaling rate to reach a minimum value at 90 rpm.

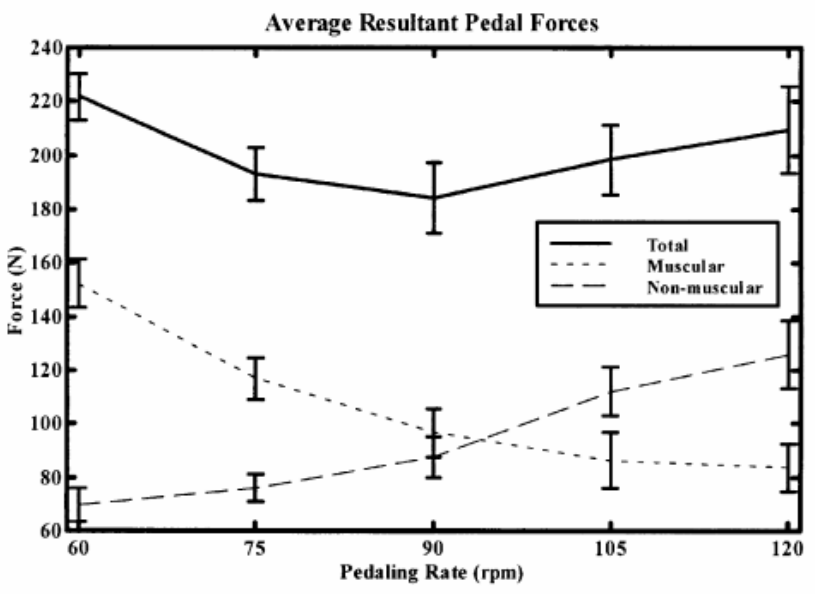

Fig 3.6 Average muscular and non-muscular pedal forces [13].

In 1999, Neptune and Hull [6] made an analysis and simulation of preferred cadence selection. They investigated neuromuscular quantities such as the individual muscle forces, stress and endurance. The results from these pedaling simulations indicated that all neuromuscular quantities are minimized at 90 rpm when summed across muscles, as shown in Fig 3.7.

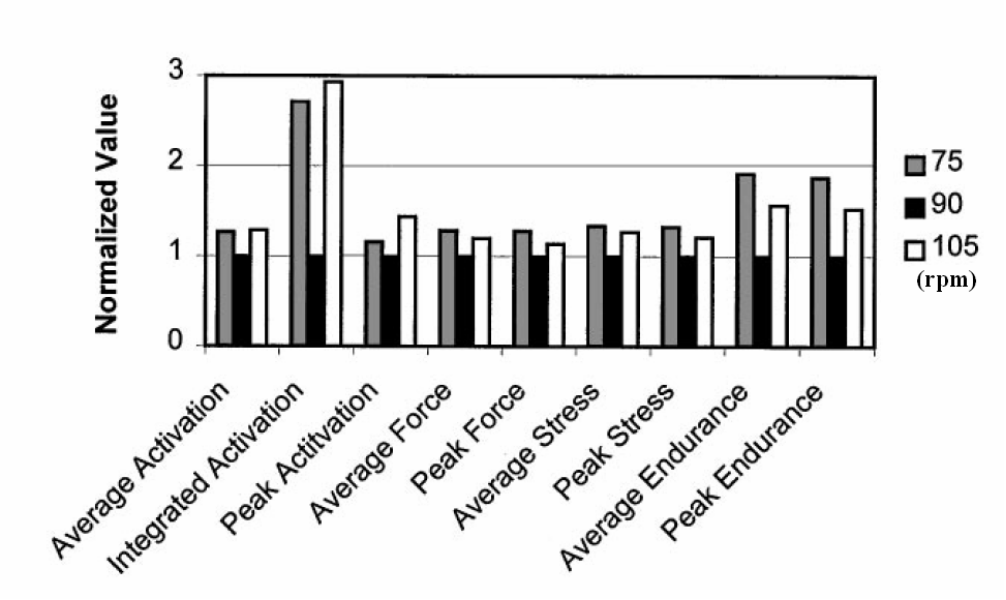

Fig 3.7 Normalized neuromuscular quantities across the different pedaling rates [6]

In 2000, Marsh, et al. [5] made an experiment about relationship between joint moment and preferred pedaling cadence. They defined a joint moment based cost function that is the sum of the average absolute joint moments at the hip, knee and ankle. They divided three groups of cyclists: trained cyclists, runners and less-trained cyclists. As shown in Fig 3.8, the cost function cadence increased as power output increased. In addition, the increases are similar for all three subject groups. In the three group, the cost function cadence is significantly higher at 150 W (93.3 ± 10.4 rpm) than at 100 W (86.3 ± 11.9 rpm). For the trained cyclists and runners groups, the cost function cadence increases from 86.3 ± 10.2 to 94.0 ± 9.6 rpm and again to 98.5 ± 8.0 rpm and decreases slightly to 96.1 ± 7.3 rpm as power output increases from 100 to 250 W. The cost function cadences of trained cyclists, runners and less-trained cyclists are not different at the two power outputs (100 and 150 W) to all three groups. The interaction between the power and the group is statistically significant. As shown in Fig 3.9 and Fig 3.10, less-trained cyclists select lower cadences at both 100 and 150 W compared to other two groups, and reduce cadence as power output increased. The results of other two groups are not different in preferred cadence and do not alter cadence as

power output increased. The cost function cadence at 200 W for cyclists and runners (101 and 96 rpm) agreed closely with previous research by Redfield and Hull who reported a cadence in the range of 90 to 105 rpm.

In summary, the conclusions from previous studies about the optimum cadence are:

1. Minimizing the joint moments can get the optimal pedal cadence ranges between 90 to 105 rpm.
2. Minimizing the muscle stress can get the optimal pedal cadence ranges between 95 to 100 rpm.
3. Minimizing the pedal force can get the optimal pedal cadence about 90 rpm.
4. The experience of riders influence the results a lot in human cycling.

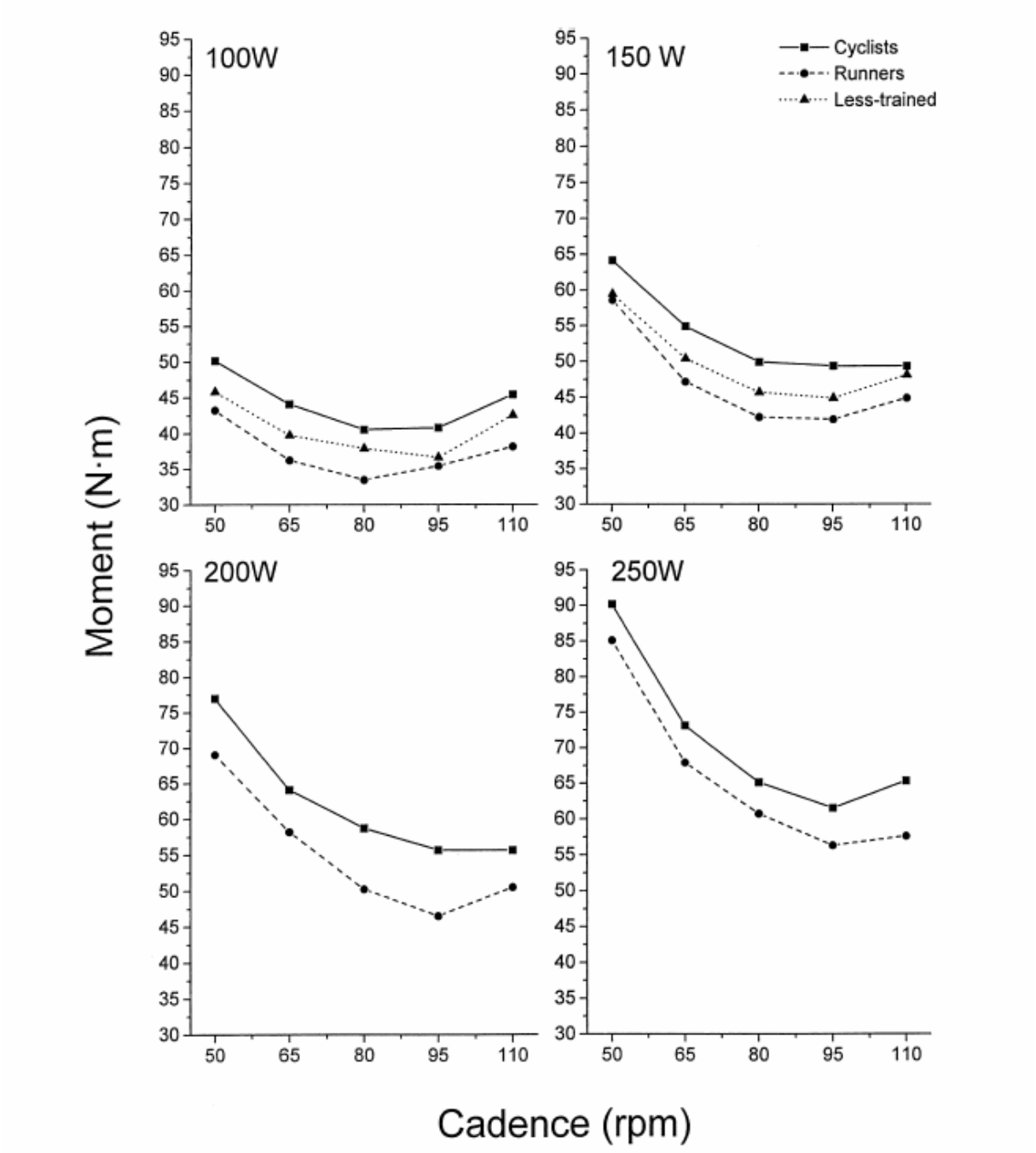

Fig 3.8 Influence of cadence and power output on the moment based cost function [5]

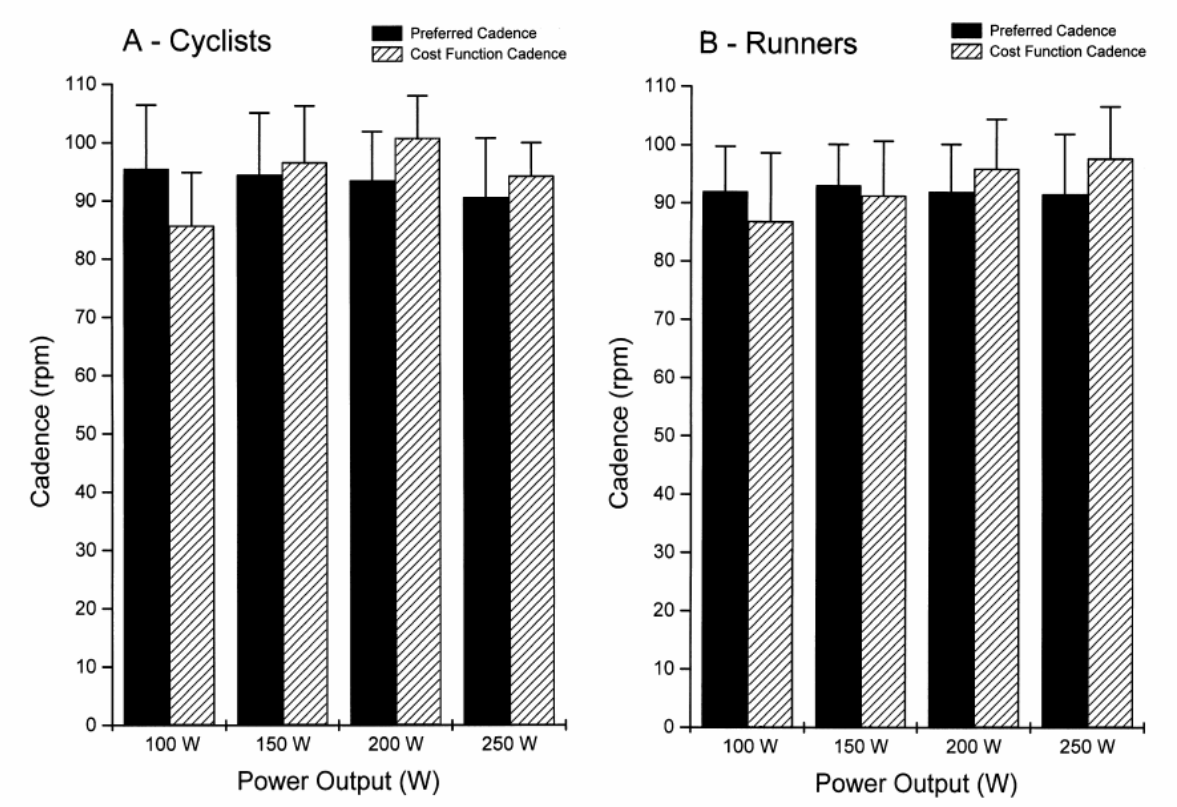

Fig 3.9 Mean preferred and cost function cadences for trained cyclist and runners [5]

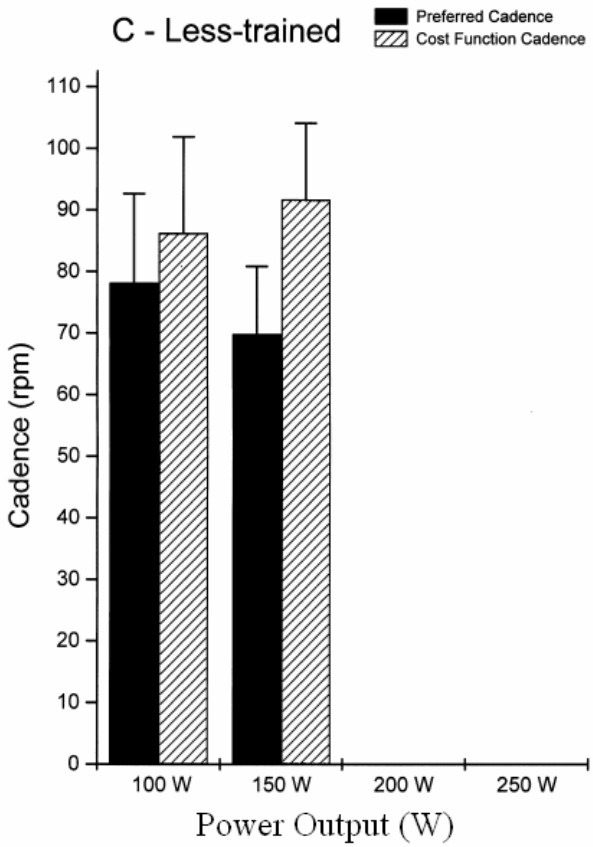

Fig 3.10 Mean preferred and cost function cadences for less-trained cyclist [5]

3.2 Cardiovascular

The cardiovascular system is an important factor when riding a bicycle. People riding bicycles will pant and his heartbeat become fast. It will make riders feel tired and uncomfortable. If a rider's cardiovascular system can endure the loading from cycling, he or she can ride for a long time. Wilson [7] indicated that everyone should be able to work easily at one-third of maximal oxygen uptake, but exceeding two-thirds of maximal oxygen uptake for a long duration may require considerable training. For a non-trained person, the maximum oxygen-absorption rate (VO_2 max) is assumed to be about 50 ml/s. When a rider is using about a third of his maximum oxygen-absorption rate, the power output is about 0.1 hp (75W). He thought that common people can work under these conditions for several hours without suffering fatigue.

In 1981, Hagberg et al. [15] made experiments to find the effect of pedaling rate on submaximal exercise responses of competitive cyclists. The road-racing cyclists used gears during the loaded cycling trials that elicited pedal cadences between 68 and 126 rpm. They measured rider's heart rate, oxygen consumption, expiratory flow, and blood lactate. And the heart rate increase, whereas net heart rate (after subtracting the heart rate during unloaded cycling) decreased with increasing pedal rate during loaded cycling. Expiratory flow, oxygen consumption and blood lactate increased much more rapidly above the optimal cadence than blow it. They found that the optimal cadence for each subject ranged from 72 to 102 rpm.

In 1993, Marsh and Martin made experiments to compare the preferred cadences and the aerobic demand response to cadence manipulation of highly fit, experienced cyclists and equally for non-cyclists [8]. They defined the most economical cadence is the cadence minimizing oxygen consumption, and the preferred cadences are freely chose cadency by riders. As shown in Fig 3.11, at constant power output of 200W, the cyclists preferred cadence is 85.2 ± 9.2 rpm and their most economical cadence is 56.1 ± 6.9 rpm. The non-cyclists preferred cadence is 91.6 ± 10.5 rpm and their most economical cadence is 62.9 ± 4.7 rpm.

They found that the preferred cadence was significantly higher than the most economical cadence for both cyclists and non-cyclists, and higher cadences produce higher oxygen consumption. Both cyclists and non-cyclists reported that they felt more comfortable at the higher cadences during 200 W cycling. And both preferred cadence and the most economical cadence of cyclists are lower than non-cyclists'. In 1999, Woolford [14] and his coworkers made experiments and found that for the same power output, maximum oxygen consumption is smaller at pedal cadences of 90~100 rpm compared with 120~130 rpm. The results here can be concluded as:

1. Riding bicycles emphasize the strength in legs more than the cardiovascular system.
2. Higher cadences make rider comfortable and can ride for a long time, but it cost more oxygen consumption.
3. Cyclists have a stronger cardiovascular system than non-cyclists, so they can use less oxygen consumption at the same cadence.

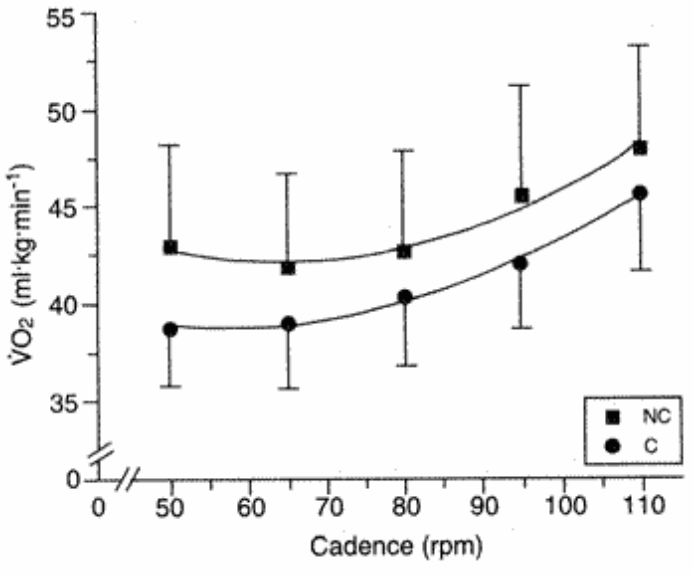

Fig 3.11 Cadence and oxygen consumption [8]

3.3 Power and torque

If a rider can maintain higher power, he or she can ride bicycle more easily. High power means using energy well. It makes riders easy to move bicycles forward. Riders generate force to make torque on the shaft of the pedals. Lower cadence leads high torque. High torque means that high angular acceleration and high pedaling forces generated. High angular acceleration can make rider get the high velocity in a short time, but high pedaling forces might break rider's body. On the contrary, high cadence generates lower torque, and it might make rider easy to feel tired.

One experiment was made to test the relationship between power output and pedal cadence [16]. As shown in Fig 3.12, the subject developed maximum power for all duration at 40 to 50 rpm and the maximum muscle efficiency was achieved at about 50 rpm. And another experiment used to find the power output an ordinary untrained cyclist could maintain over useful periods of time. The results showe in Fig 3.13, for prolonged periods about 0.05 hp was maintained with pedaling rates of 20 to 60 rpm.

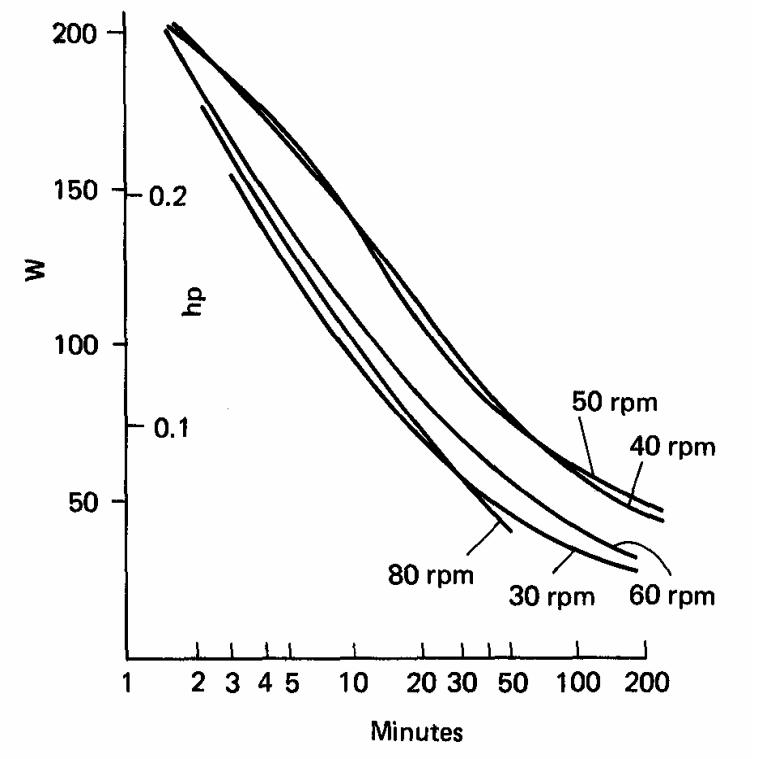

Fig 3.12 Pedaling power versus time [16]

speed to torque.

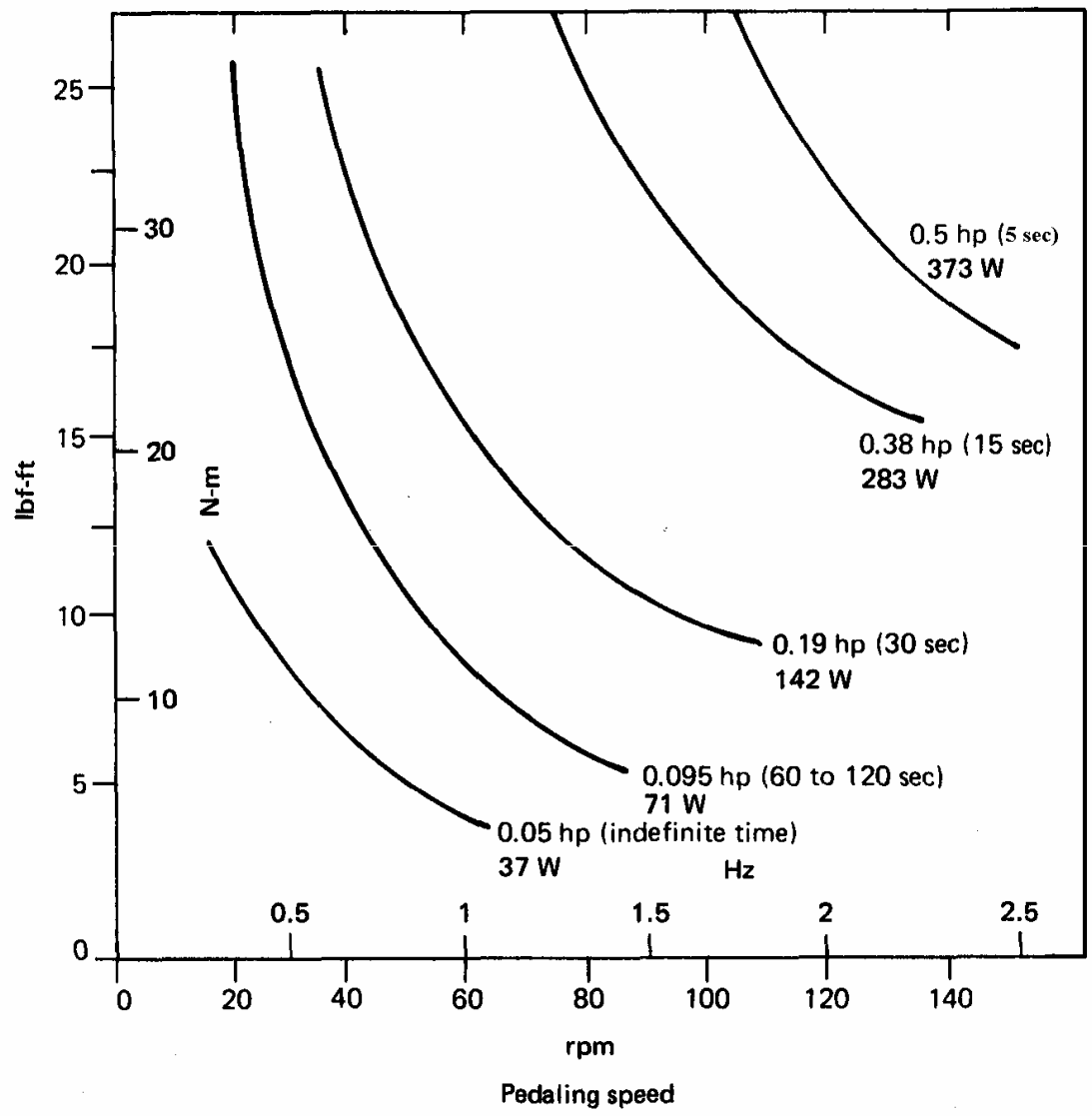

Fig 3.13 Relationship of pedaling speed to torque [16]

In 1997, Martin [17] and his coworkers demonstrated that instantaneous cycling power-velocity and torque-velocity relationships across a range of pedaling rates from a single exercise. They measured the instantaneous power (P_I) and computed the average power (P_{REV}). As Fig 3.14 and Fig 3.15 shown, maximum value of P_{REV} is 1317 ± 66 W and can be achieved at a pedaling rate of 122 ± 2 rpm. Maximum value of P_I averaged is 2137 ± 101 W and occurres at a pedaling rate of 131 ± 2 rpm. They also measured the instantaneous torque (T_I) and computed the average torque (T_{REV}) as Fig 3.16 shown. The result matches with Fig 3.17 reported by Wilson [7]. He indicated that some people produce maximum power at 120 rpm and can spin up to 180 rpm, whereas others can manage only half these speeds. These results can be concluded as:

1. High pedaling cadence is not totally good for human power.
2. The relationship between human power and torque conforms to the theory.

There is a lot optimal pedaling cadence based on different view points. The prior researches results mentioned above can provide the data as shown in Table 3.1. From these results, this study takes the optimal pedaling cadence range is between 60 to 90 rpm. The range will be the criterion of the new gear-shifting strategy.

Table 3.1 Optimal pedaling cadence range based on various view point

Optimal variables	Optimal pedaling cadence range (rpm)	The mean pedaling cadence (rpm)
VO2	72~102	87
Neuromuscular	65~105	85
Forces	75~105	90
Joint moment	89~103	96
Cardiovascular	49~63	56
Power	120~124	122
Muscle stress	95~100	97.5

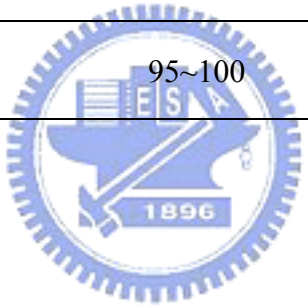

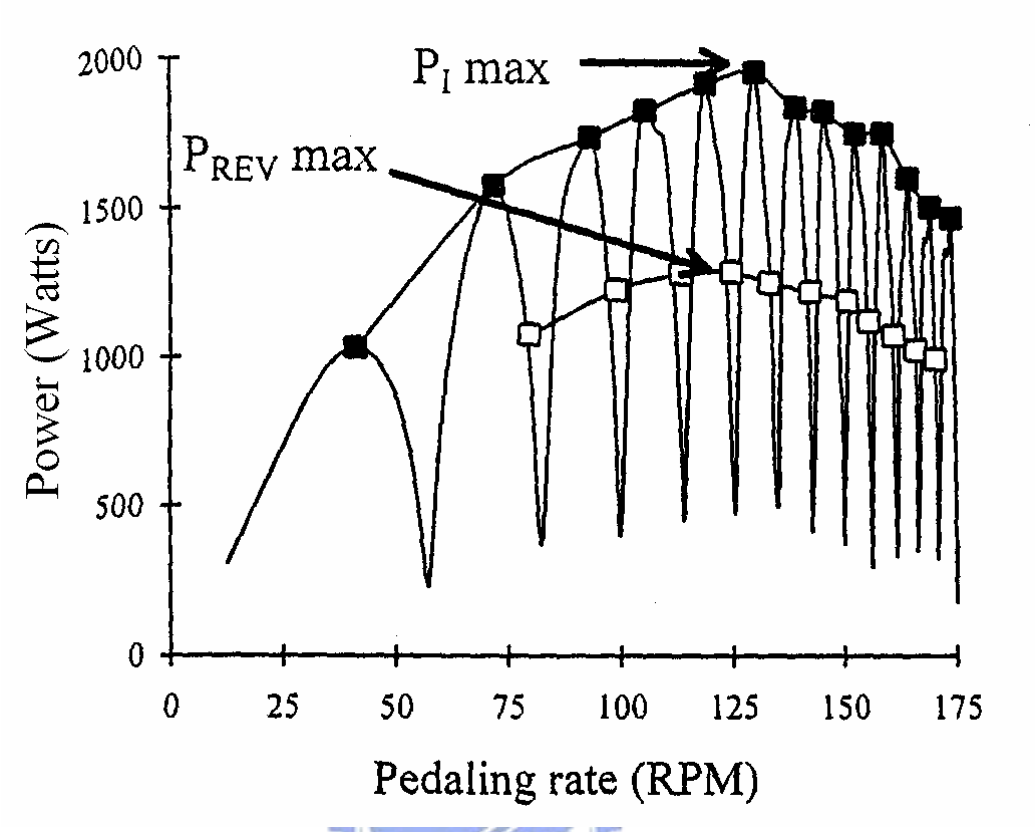

Fig 3.14 Pedaling rate and power [17]

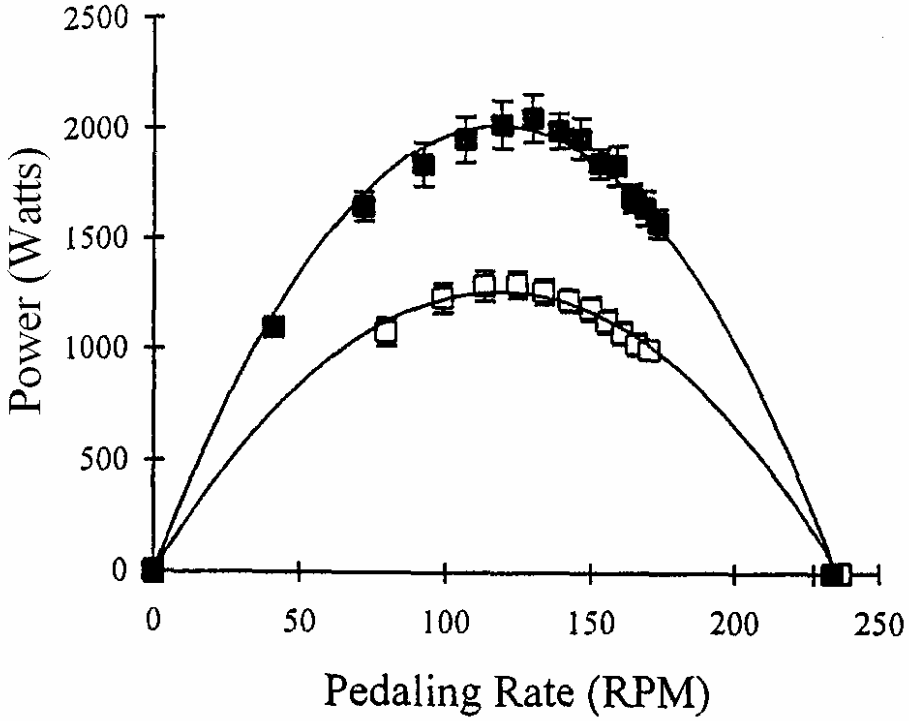

Fig 3.15 Mean power-velocity relationship [17]

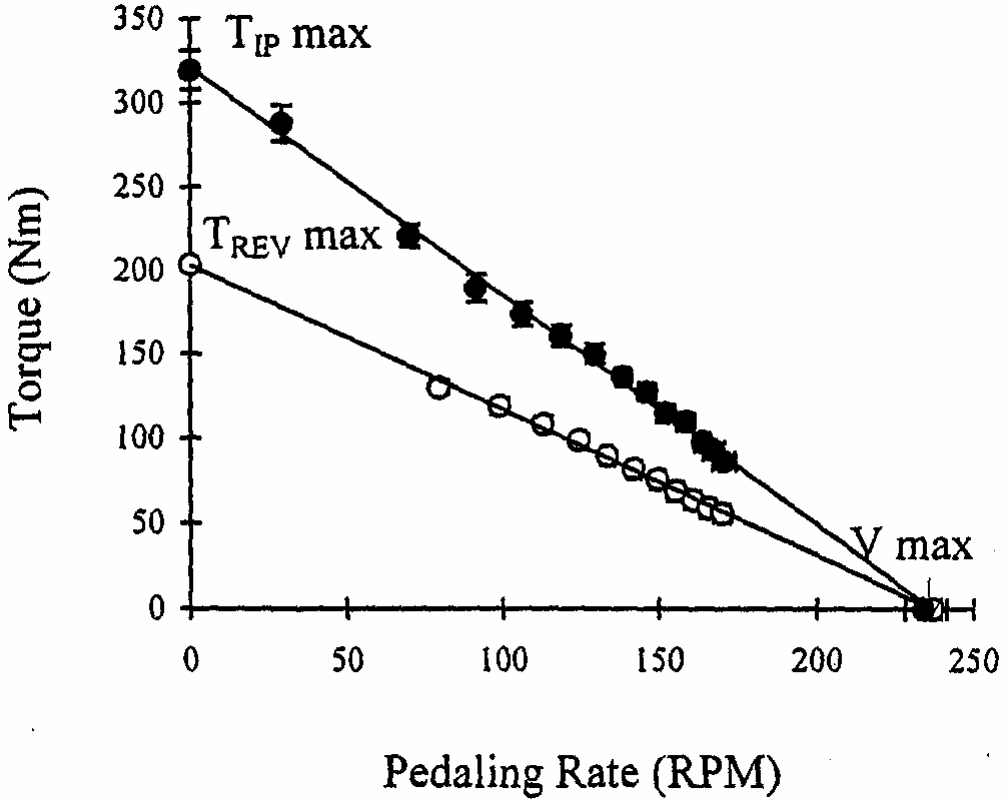

Fig 3.16 Mean torque and pedaling rate [17]

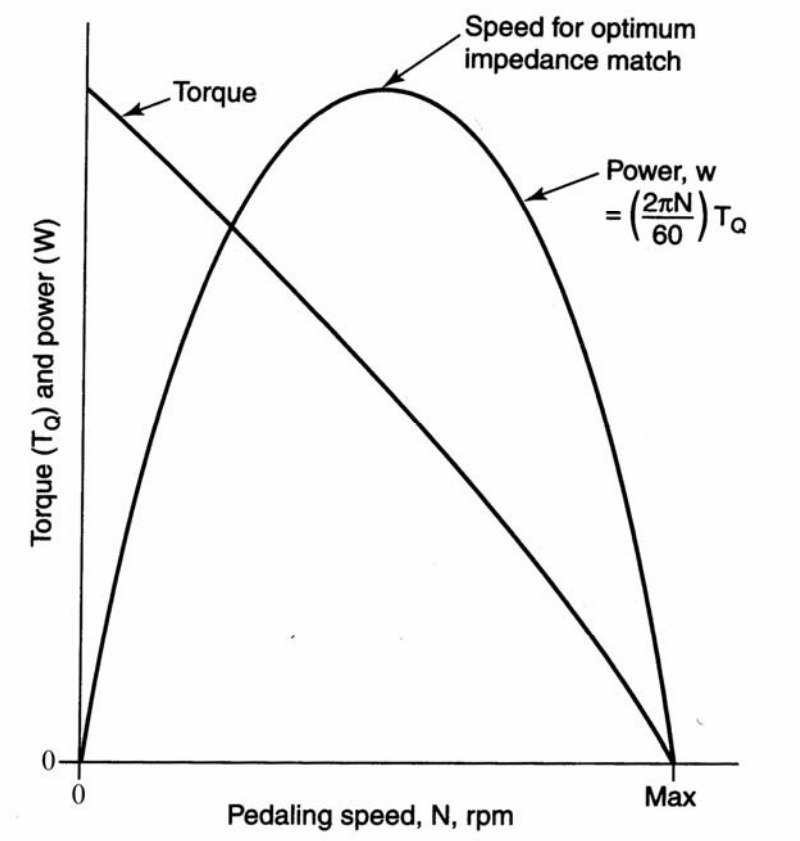

Fig 3.17 Torque and power versus pedaling speed [7]

CHAPTER 4

FUZZY LOGIC CONTROLLER

4.1 Preliminary

From the conclusions of previous chapters, it is obvious that many factors affect human cycling, and it is difficult to obtain an unique criteria for the optimum cadence. Therefore, this study then uses the fuzzy logic controller to simulate human reasoning during cycling. Fuzzy logic first was introduced by Professor Lotfi Zadeh in 1965 [18]. It can be extremely useful not only in engineering and technological sciences, but also in social sciences, eliminating the difference in the approaches between natural and social sciences. The fuzzy logic controller is a tool for processing a fuzzy form of information in a nonfuzzy or fuzzy scheme of reasoning. It have some advantages as follows [19]:

- Ability to translate imprecise/vague knowledge of human experts
- Simple to implement technologies
- Software design and hardware implementation widely support
- Results are easy to transfer from product to product
- Smooth and robust controller behavior
- Ability to control unstable systems

As shown in fig 4.1, a simple fuzzy logic controller contains a fuzzification interface, a fuzzy knowledge base, an inference engine, and a defuzzification interface.

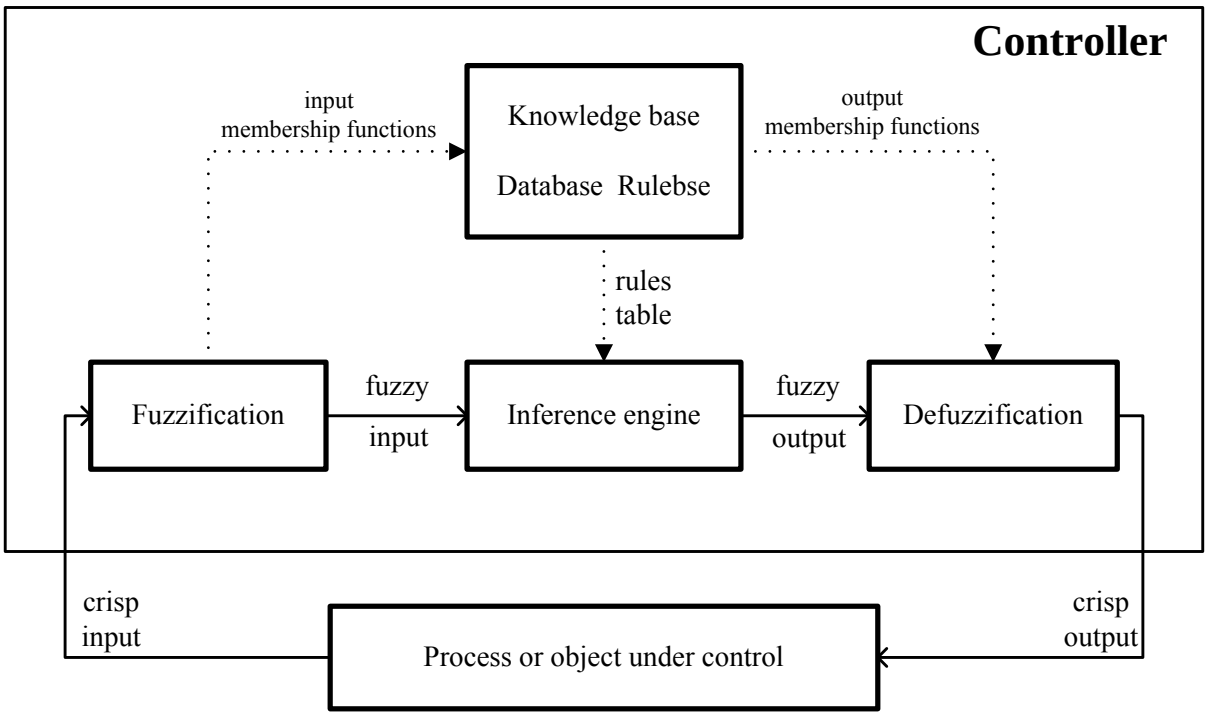

Fig 4.1 The fuzzy logic controller (a basic structure)

4.2 Fuzzification

The fuzzificaton interface can get data from data acquisition interface. This process will define fuzzy sets and develop membership functions. It is the process of making a crisp quantity into a fuzzy quantity.

A fuzzy set is a set containing elements that have varying degrees of membership in the set. It is in contrast with classical or crisp sets because members of a crisp set would not be members unless their membership was full or complete in that set. Elements of a fuzzy set are mapped to a universe of membership values using a function-theoretical form. For example, let set **A** be a fuzzy set. This function maps elements in a fuzzy set **A** to a real numbered value on the interval [0,1]. If an element in the universe of discourse, say *x*, is a member of fuzzy set **A**, then this mapping is given by

$$\mu_A(x) \in [0,1] \tag{4.1}$$

The symbol $\mu_A(x)$ is the degree of membership of element *x* in the fuzzy set **A**. Therefore, $\mu_A(x)$ is a value on the unit interval that measures the degree to which element *x* belongs to

the fuzzy set **A**. The function $\mu_A(x)$ is the membership function that embodies the mathematical representation of membership in a set.

This mapping is shown in Fig 4.2 for a typical fuzzy set. When the universe of discourse, *x*, is discrete and finite, a notation convention for fuzzy sets is

$$A = \left\{ \frac{\mu_A(x_1)}{x_1} + \frac{\mu_A(x_2)}{x_2} + \ldots \right\} = \left\{ \sum_i \frac{\mu_A(x_i)}{x_i} \right\} \tag{4.2}$$

Fuzzy sets follow the same properties as crisp sets. Because the membership values of a fuzzy set in [0,1] are a subset of the real values, fuzzy sets can be thought of a special case of classical sets.

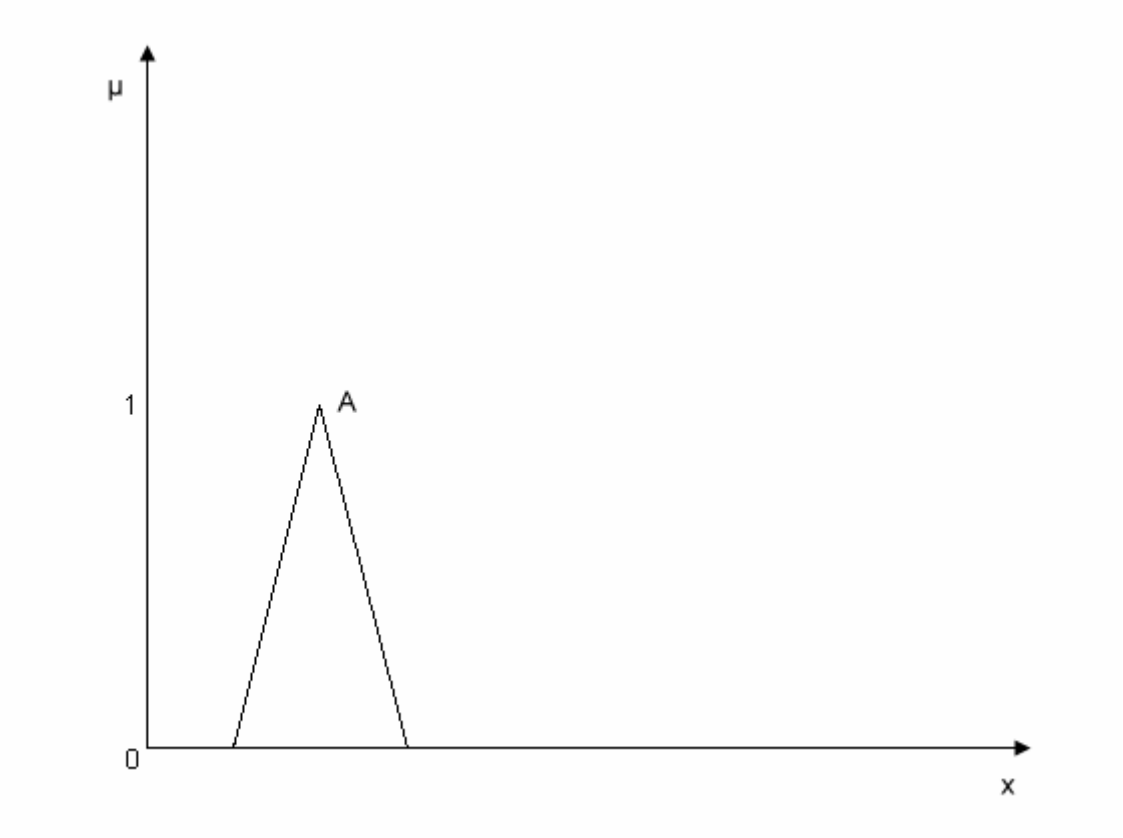

Fig 4.2 Membership function for fuzzy set A

4.3 Fuzzy Knowledge Base

The knowledge base of a fuzzy logic controller consists of a knowledge base and a rule base. The basic function of the knowledge base is to provide the necessary information for the proper functioning of the fuzzification interface, the rule base and the defuzzification interface. This information includes:

1. Fuzzy sets representing the meaning of the linguistic values of the process state and control output variables.
2. Physical domains and their normalized counterparts together with the normalization / denormalization (scaling) factor.

The basic function of the rule base is to represent in a structured way by the control policy of experienced process operators in the form of a set of production rules such as:

If (process state) *then* (control output) (4.3)

The *if*-part of such a rule is called the rule-antecedent and is a description of a process state in terms of a logical combination of atomic fuzzy propositions. The *then*-part of the rule is called the rule-consequent and is again a description of the control output in terms of a logical combination of fuzzy propositions. These propositions state the linguistic values which the control output variables take whenever the current process state matches the process state description in the rule-antecedent.

4.4 Inference

The basic function of the inference engine is to compute the overall value of the control output variable. This process will be completed by defining fuzzy relations and fuzzy compositions. Fuzzy relations also map elements of one universe, say *x*, to those of another universe, say *y*, through the Cartesian product of the two universes. Let **A** be a fuzzy set on universe *x* and **B** be a fuzzy set on universe *y*; then the Cartesian product between fuzzy sets **A** and **B** will result in a fuzzy relation ***R***, which is contained within the full Cartesian product space. The Cartesian product defined by Eq (4.4) or Eq (4.5), which is implemented in the same fashion as is the cross product of two vectors.

$$A \times B = R \subset X \times Y \tag{4.4}$$

Where the fuzzy relation R has membership function

$$\mu_R(x,y) = \mu_{A\times B}(x,y) = \min[\mu_A(x), \mu_B(y)] \tag{4.5}$$

There are many fuzzy composition methods to computer. The followings are those proposed in the literature for the composition operation **B**=**A** • ***R***, where **A** is the input, or antecedent defined on the universe *x*, **B** is the output, or consequent defined on universe *y*, and ***R*** is a fuzzy relation characterizing the relationship between specific input (*x*) and specific outputs (*y*) :

Max-min: $$\mu_B(y) = \max_{x\in X}\{\min[\mu_A(x), \mu_R(x,y)]\} \tag{4.6}$$

Min-max: $$\mu_B(y) = \min_{x\in X}\{\max[\mu_A(x), \mu_R(x,y)]\} \tag{4.7}$$

Max-max: $$\mu_B(y) = \max_{x\in X}\{\max[\mu_A(x), \mu_R(x,y)]\} \tag{4.8}$$

Min-min: $$\mu_B(y) = \min_{x\in X}\{\min[\mu_A(x), \mu_R(x,y)]\} \tag{4.9}$$

4.5 Defuzzification

Defuzzification is the conversion of a fuzzy quantity to a precise quantity whereas fuzzification is the conversion of a precise quantity to a fuzzy quantity. The output of a fuzzy process can be the logical union of two or more fuzzy membership functions defined on the universe of discourse of the output variable. There are several methods for defuzzification:

1. *Max membership method*: This is known as the *height* method, and it is limited to peaked output functions. This method is given by the following expression

$$\mu_C(z^*) \geq \mu_C(z) \quad \text{for all} \quad z \in Z \tag{4.10}$$

where z^* is the defuzzified value, and it is shown in Fig 4.3

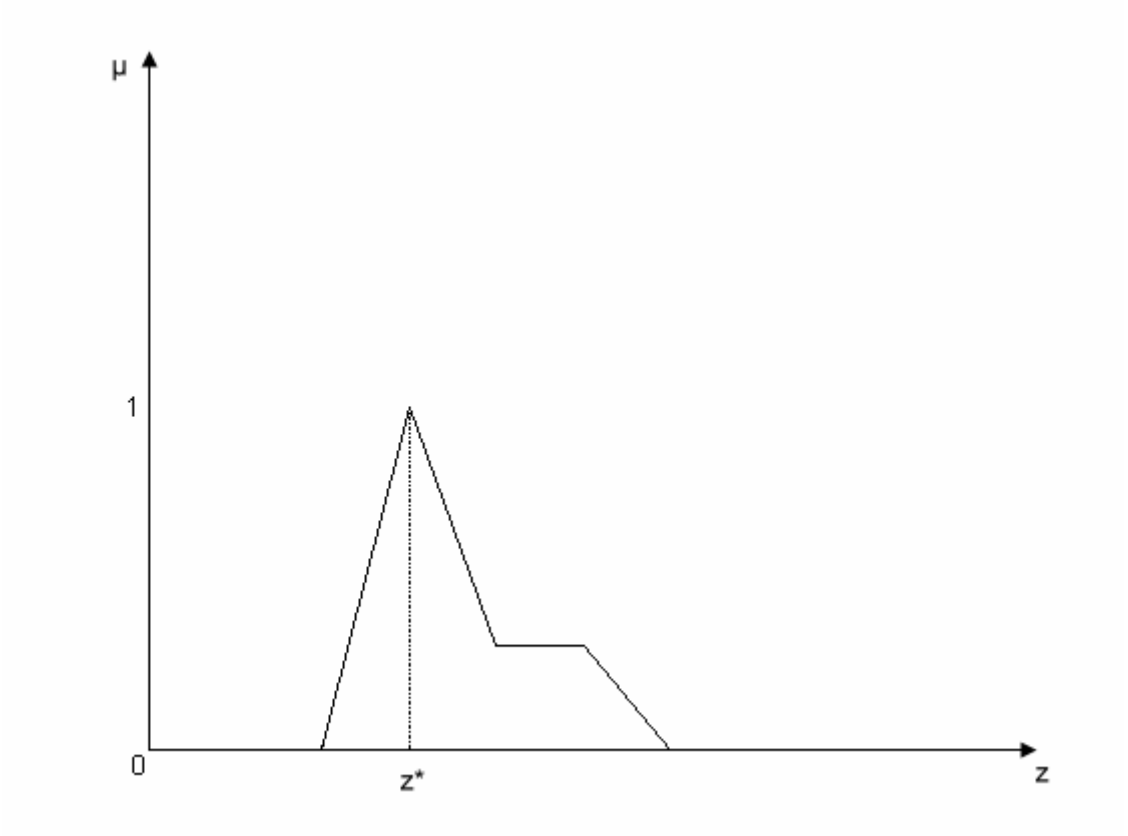

Fig 4.3 Max membership defuzzification method

2. *Centroid method*: this procedure (also called center of area or center of gravity) is the most prevalent and physically appealing of all the defuzzification methods. It is given by:

$$z^* = \frac{\int \mu_C\left(\bar{z}\right) \bullet z dz}{\int \mu_C(z) dz} \tag{4.11}$$

where $\int$ denotes an algebraic integration. This method is shown in Fig 4.4

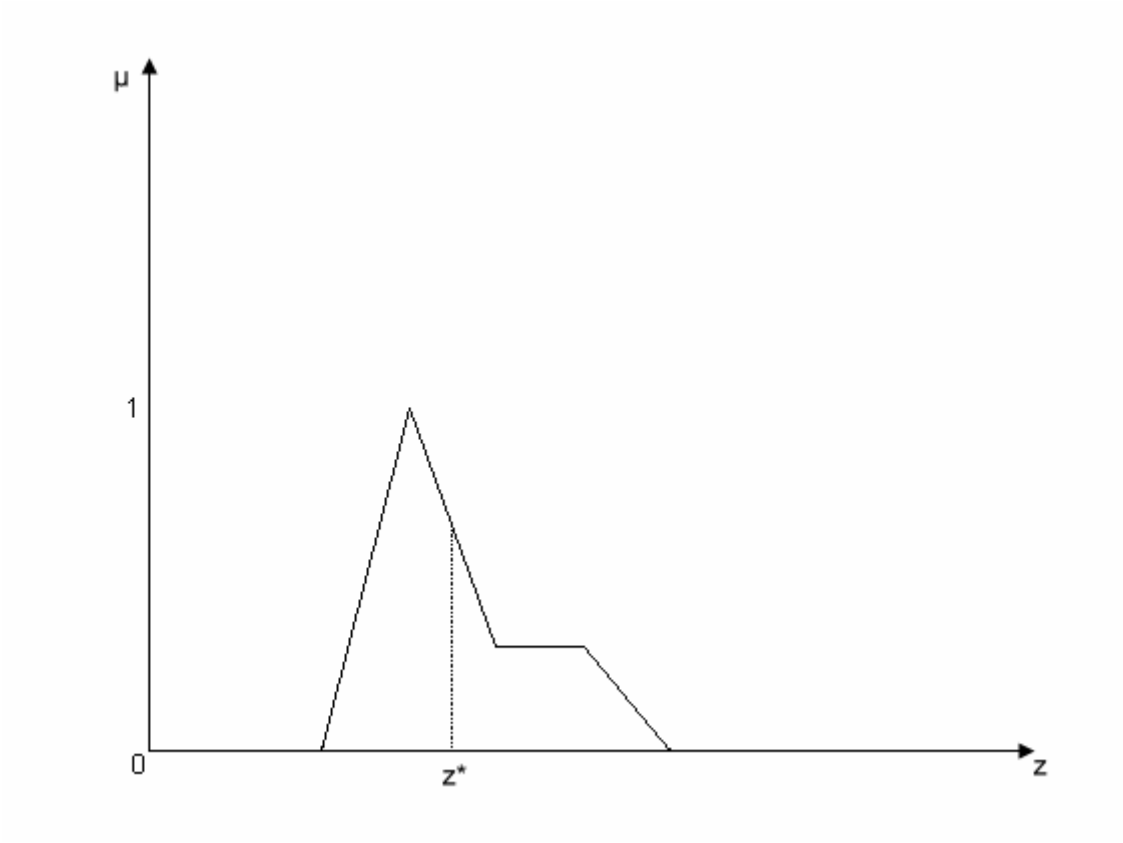

Fig 4.4 Centroid defuzzification method

3. *Mean max membership method*: This method is closely related to max membership method, expect that the location of the maximum membership can be nonunique. This method is given by the expression:

$$z^* = \frac{a+b}{2} \tag{4.12}$$

where *a* and *b* are defined in Fig 4.5

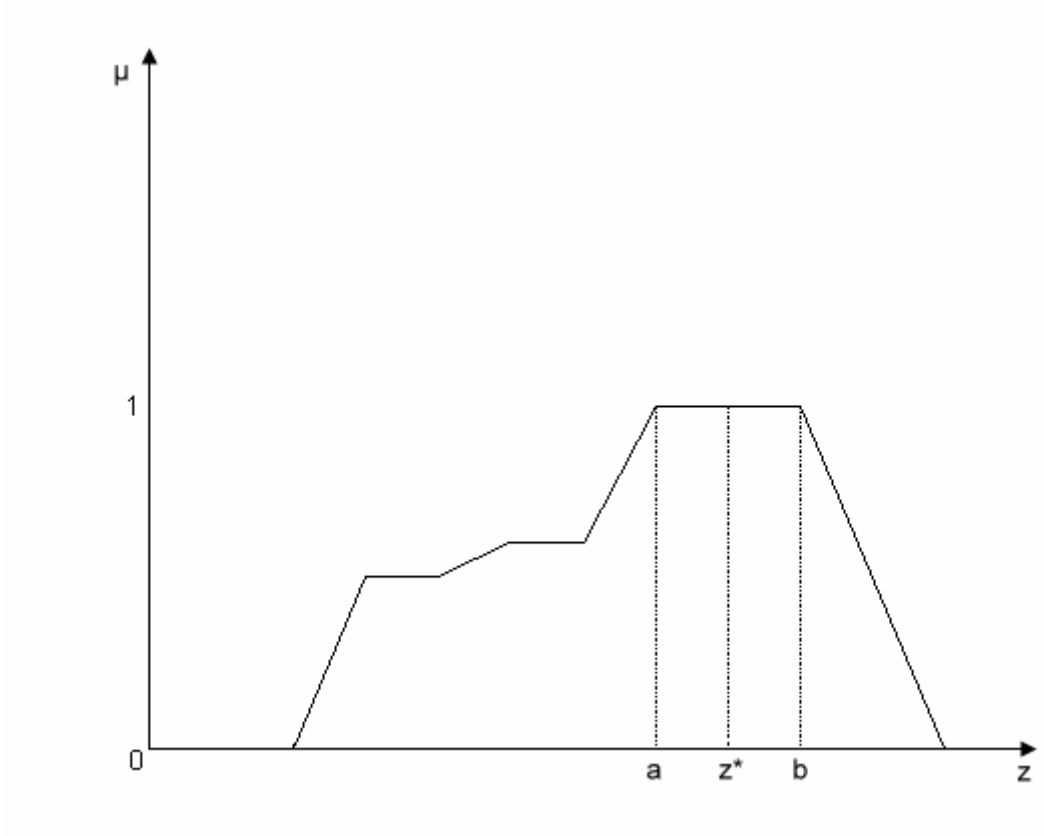

Fig 4.5 Mean max membership defuzzification method

4.6 Apply Fuzzy Logic Controller to Gear-Shifting Control

As mentioned in Chapter 3, there are many researches mentioned the optimal pedal cadence range based on various viewpoints as shown in Table 3.1. It is obvious that the ranges represent fuzz sets.

According to these results, this study chooses the this pedal cadence range to construct the fuzzy set and the membership functions of the pedal cadence and velocity. Riders can feel comfortable riding in this range because it costs small loading of forces, muscle stress, joint moment, neuromuscular, and VO_2.

Following the procedures can get an easy fuzzy logic controller. It needs to set the membership function, construct the *if-then* rule base, choose the inference method, and the defuzzification method. This paper uses two input variables, velocity (v) and pedal cadence (u), and one output variable, gear-ratio (g). The fuzzy set and membership function of the velocity $\mu_V(v)$ with the degree about small, medium, and fast is shown in Fig 4.6. Fig 4.7 and Fig 4.8 show the sets of the pedaling cadence $\mu_U(u)$ and the gear ratio $\mu_G(g)$. The membership functions defined here can be modified by considering various variables. After this process, the input variables can be transferred to linguistic variables, and the output variables are transferred from linguistic ones to quantitative ones.

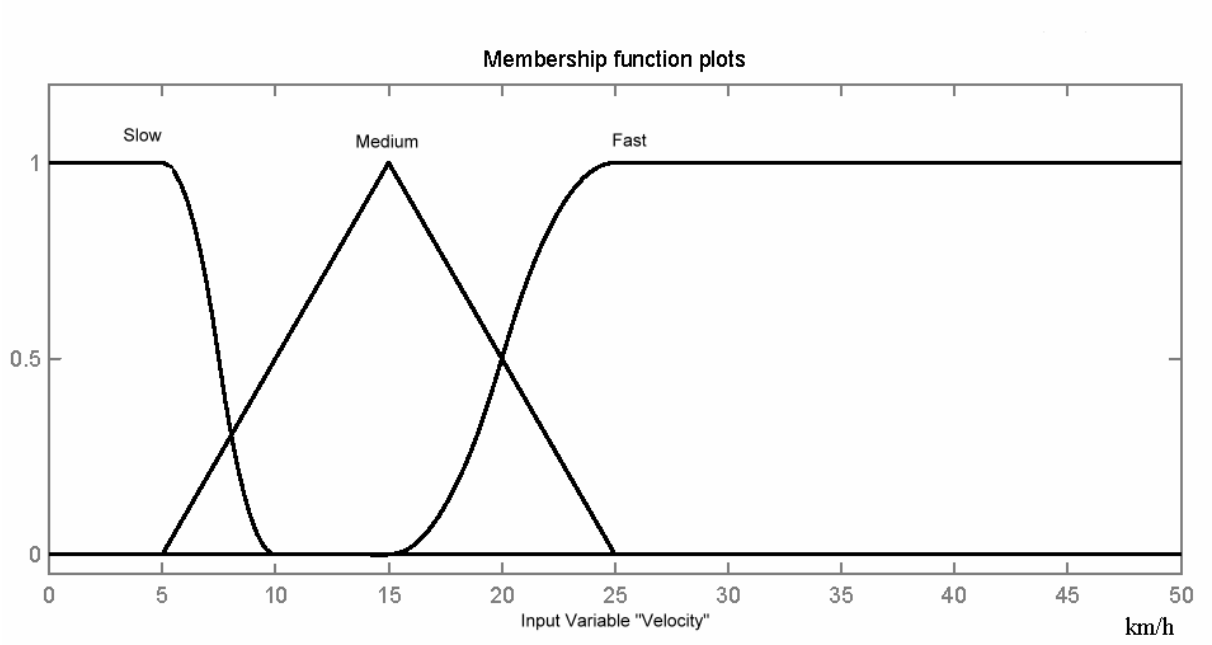

Fig 4.6 Membership function of velocity

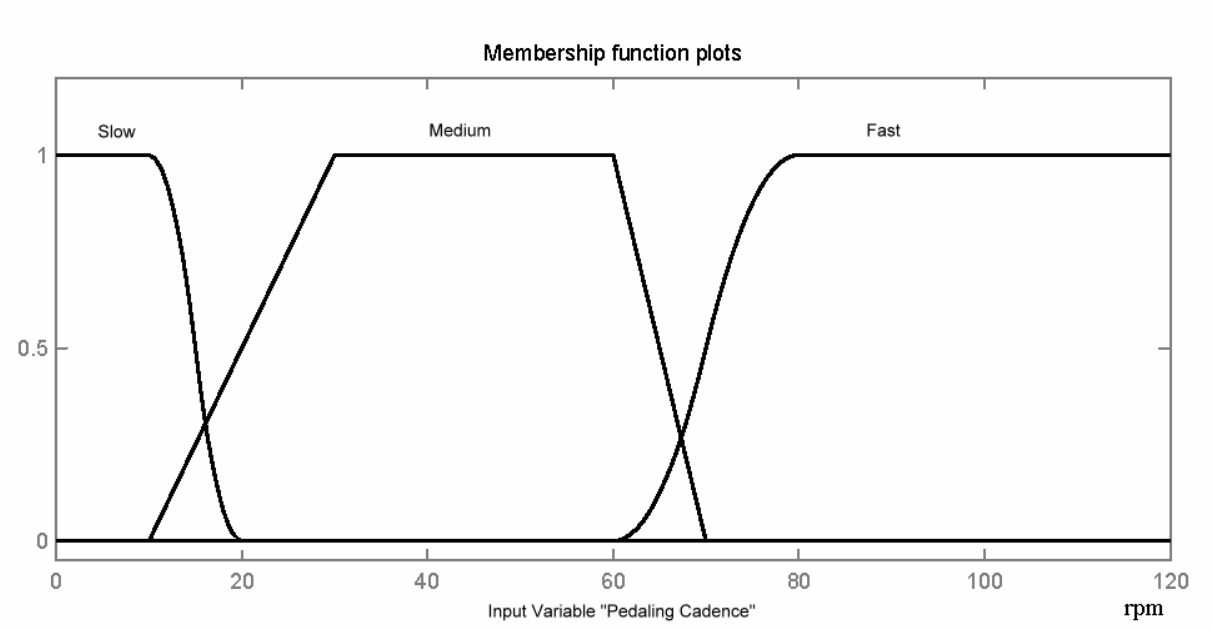

Fig 4.7 Membership function of pedal cadence

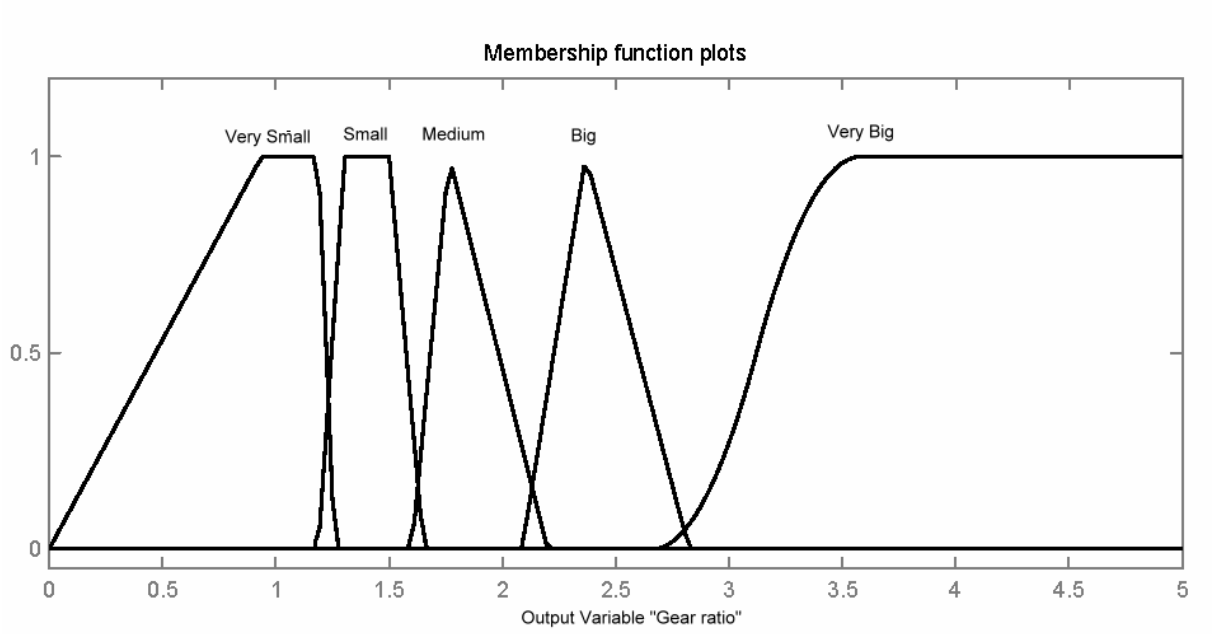

Fig 4.8 Membership function of gear-ratio

Because there are two inputs and one output variables, nine fuzzy rules can be constructed as shown in Table 4.2. The general form of the rules in this case of two-input-single-output system is:

R^i: IF (v is V_i) AND (u is U_i), THEN (g is G_i) , i=1 to 9. (4.13)

where v, u and g are linguistic variables representing the velocity, pedal cadence and gear raio, respectively. V_i , U_i and G_i are the linguistic values of the variables v, u and g.

Take the rule 3 in Table 4.2 for example, if the input velocity is slow and pedal cadence is fast, it means that the gear ratio is small at the moment, and the pedal cadence is too fast. Therefore, the output gear ratio should be change to a medium one in order to lower the pedal cadence and increase the velocity. Fig 4.9 shows the response surface that represents the mapping from the input to the output according the fuzzy rules.

Table 4.1 Fuzzy rule base

Rule #	IF		THEN
	Velocity (v)	Pedal cadence (u)	Gear-ratio (g)
1	Slow	Slow	Very Small
2	Slow	Medium	Small
3	Slow	Fast	Medium
4	Medium	Slow	Small
5	Medium	Medium	Medium
6	Medium	Fast	Big
7	Fast	Slow	Medium
8	Fast	Medium	Big
9	Fast	Fast	Very Big

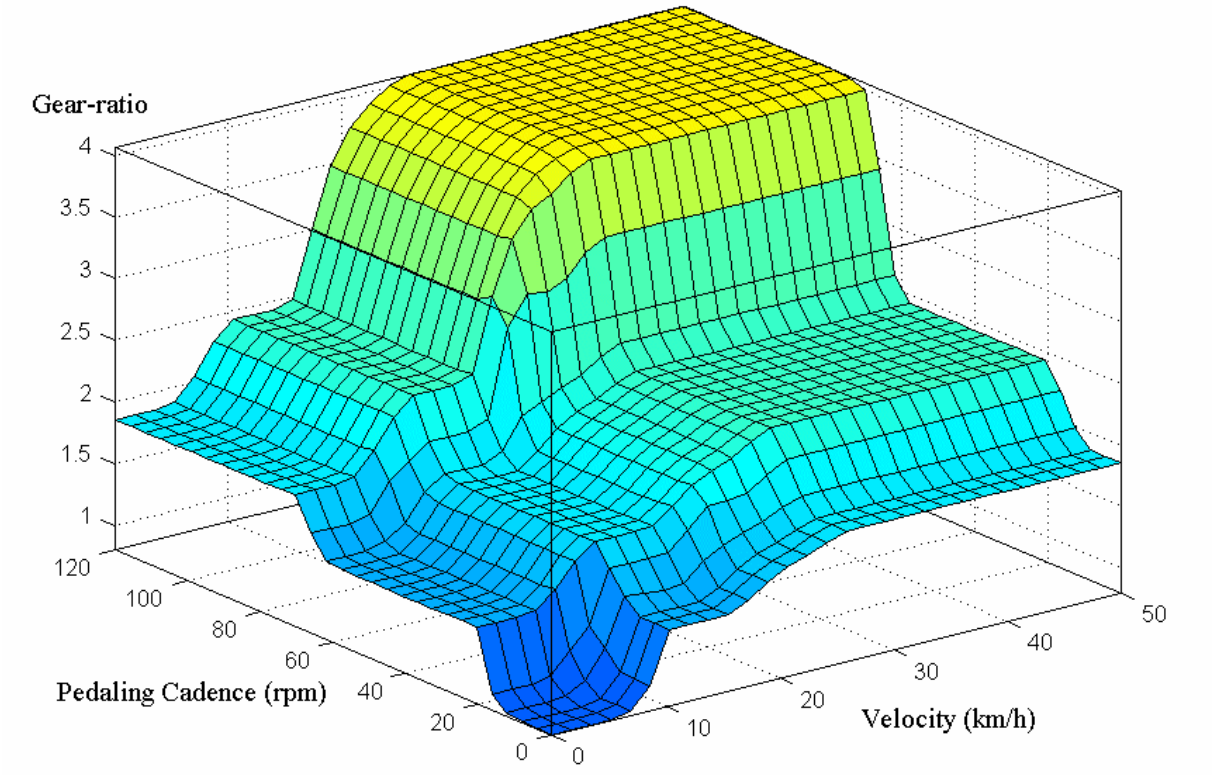

Fig 4.9 Pedal Cadence, velocity and gear ratio

This study used the max-min composition as the inference method. It is the most famous one and suitable for allt situations. Since the fuzzy rule base consists of compositional relations of inference: $R = (V \cap P) \rightarrow G$, the max-min composition is used as the fuzzy implication. Take the nine rules in Table 5.1 for example, the "IF" side is taken the "AND (MIN)" operation as shown in the following equations:

$$\mu_{G_i}(g) = \mu_{V_i}(v) \cap \mu_{U_i}(u), \text{ i=1 to 9} \tag{4.14}$$

And the final inferred consequent *G* according to the "OR (MAX)" operation are shown in the following equations:

$$\mu_G(g) = \mu_{G_1}(g) \cup \mu_{G_2}(g) \cup \mu_{G_3}(g) \cup .... \cup \mu_{G_9}(g) \tag{4.15}$$

Finally, the center of area (COA) method is selected as the defuzzification strategy. The operation is shown in the following equation:

$$g^* = \frac{\int_g \mu_G(g) g dg}{\int_g \mu_G(g) dg} \tag{4.16}$$

This method determines the center of area (g^*) below the combined membership function. The center of area means the desired gear ratio. It can be compared to the current one. If the desired gear-ratio is larger, it means the fuzzy logic controller suggests a larger gear-ratio than the current one. Therefore, a up-shifting command must act on the derailleur system, then, a larger gear-ratio can be obtained.

CHAPTER 5

CONTROL DESIGN AND EXPERIMENTS

5.1 Software

5.1.1 LabVIEW

In order to implement the proporsed fuzzy logic controller, PC based architecture is used for the hardware, and LabVIEW is selected for developing the software. LabVIEW graphical interface has revolutionized the development of scalable test, measurement, and control applications for more than 20 years. Regardless of experience, engineers and scientists can rapidly and cost-effectively interface with measurement and control hardware, analyze data, share results, and distribute systems. The key benefits of LabVIEW are described as follows:

- Graphical programming
- Bulit-in measurement and analysis functions
- High-level development tools
- Multiplatform and embedded devices

The most important thing is that LabVIEW have the tool-kit for the fuzzy logic controller design, and it is easy to use. Based on these reasons, LabVIEW is selected to be the simulation software for completing the system quickly and successfully.

5.2 Hardware

5.2.1 Browning SmartShift

Browning SmartShift is a 12-speed automatic transmission bicycle. The critical feature that differentiates the Browning System from other derailleur systems is its continuous gear/chain engagement during shifting. There is no skipping or grinding even under the heavy loads. The transmission will shift under any combination of speed, cadence and pedaling force. The chain stays fully in contrast with the gear teeth during either up-shifting or down-shifting. Another unique feature of Browning system is that it is ideally suited for complete electric operations, including computer controlled automatic shifting. It was designed for “to get on and ride”. There are two operation modes on the system. In the manual mode, riders can direct control the up-shifting or down-shifting according to road conditions. In the automatic mode, the computer controls the shifting actions according to the build-in algorithm.

Browning SmartShift includes six components as shown in Fig 5.1, 5.2, and 5.3. These components are a electric control unit (ECU), a selector assembly, control buttons & cables, sprocket clusters, a compensator, and magnets. Riders can use the toggle switch on the control button to switch the operation modes, and use the control button to change gears in the manual mode. The ECU has batteries, a center processing unit (CPU), and memories. In the manual mode, the ECU gets signals from the control buttons and sends it to the selector assembly. In the automatic mode, the ECU computes and decides a suitable gear-ratio, and controls the selector assembly to shift gears. The selector receives the signals from the ECU and guides the chain to a desired position. There are sensors for measuring the velocity and the pedaling cadence. The compensator maintains the tension of the chain by a spring, and keeps about 180 degrees of chain wrap around the sprocket at all times. The tooth numbers of the three-speed front chainwheels are 48, 38 and 30, and the four-speed rear cluster are 12, 17, 23, and 32. The magnets on the rear wheel are 180 degrees apart. It can actuate the sensors in rear and front selectors.

Fig 5.1 Browning SmartShift System

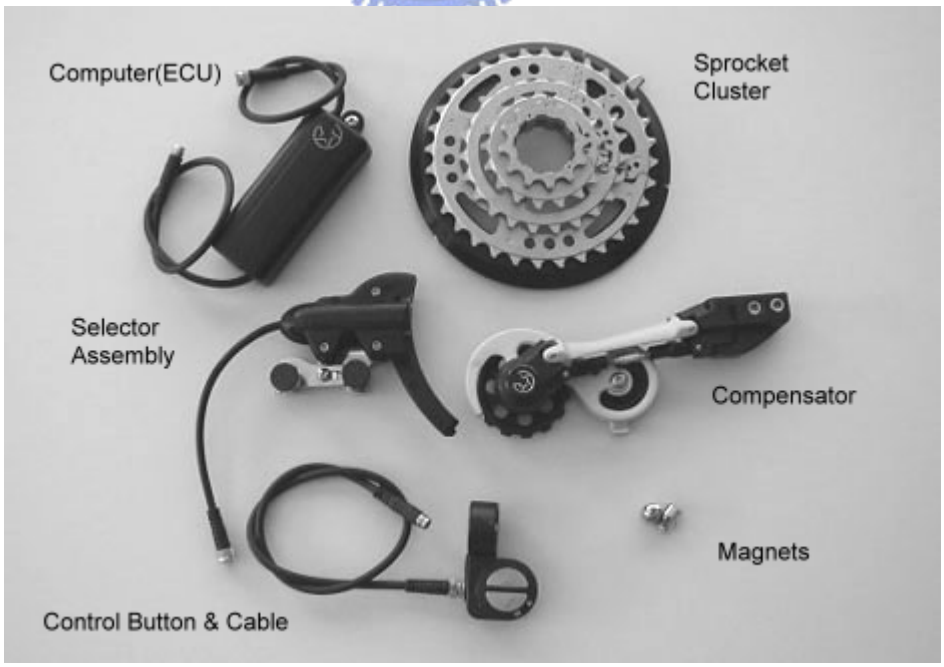

Fig 5.2 Browning SmartShift Components

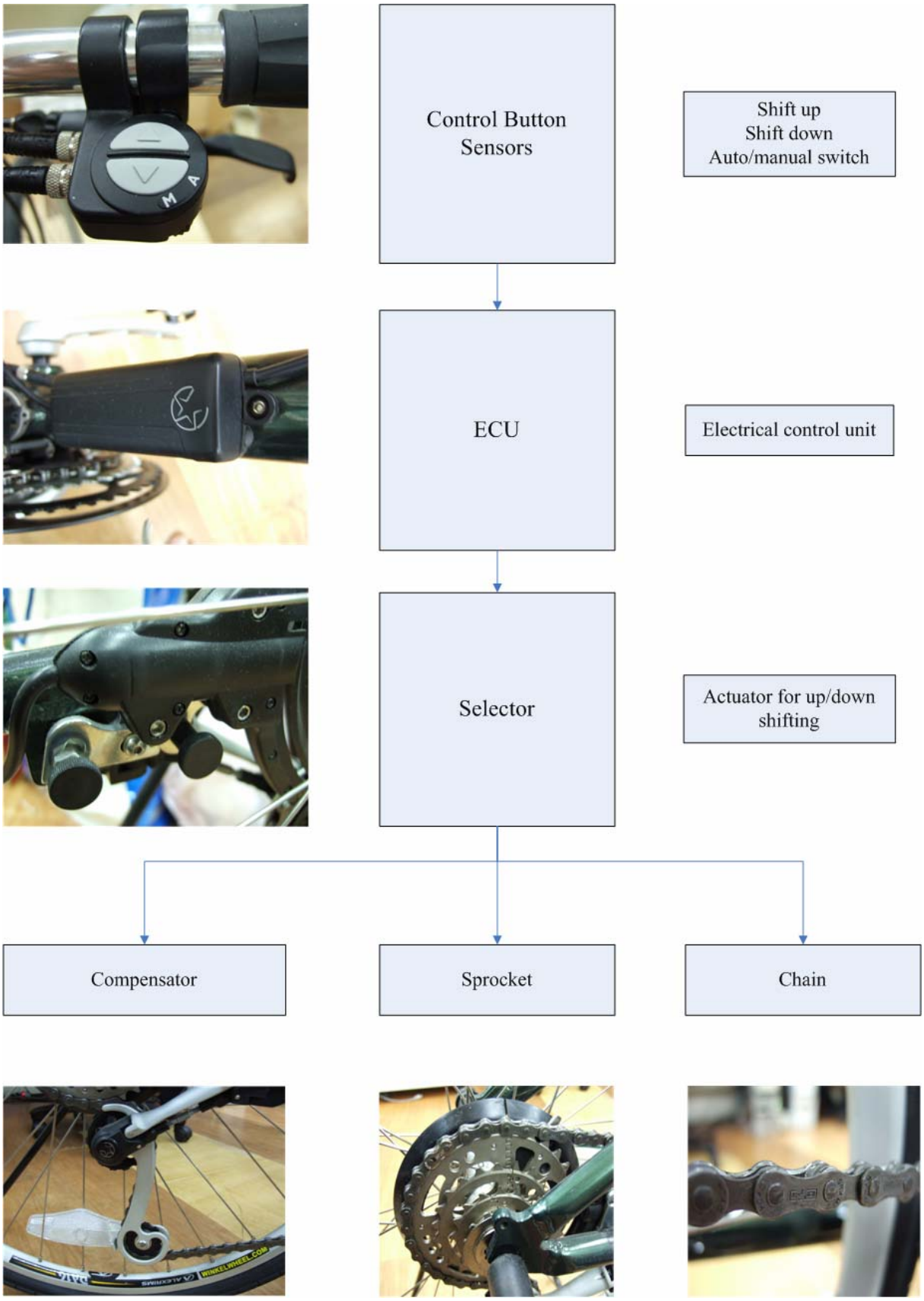

Fig 5.3 Flow chart of the Browning SmartShift actions

5.2.2 Sensors

The velocity sensor, shown in Table 5.1, is a magnetic reed switch. It actuates when magnets approach and leave. This switch is featured that it has both “normally close” and “normally open” contacts.

Table 5.1 The Velocity Sensor

Action	Normally Closed & Normally Open
Maximum Gap (cm)	3
Mounting Hole Centers (cm)	5.4
Terminal Type	Screw
Type	SPDT

The pedaling cadence sensor, shown in Table 5.2, is a simple magnetic reed switch. It switches on when magnets approach and switches off when magnets leave.

Table 5.2 The Pedaling Cadence Sensor

Action	Normally Open
Maximum Gap (cm)	2
Mounting Hole Centers (cm)	2.5
Type	SPST

5.3 System Simulations

5.3.1 Control Prototype

After completing the fuzzy logic controller, it needs to choose the gear-shifting sequence. In 2007, Lin et, all [20] developed a gear-shifting sequence to produce the minimum power change during gear-shifting, the example for a traditional 24-speed bicycles is shown in Fig 5.4. Taking it on the Browning SmartShift system can get the optimum gear-shifting as shown in Fig 5.5.

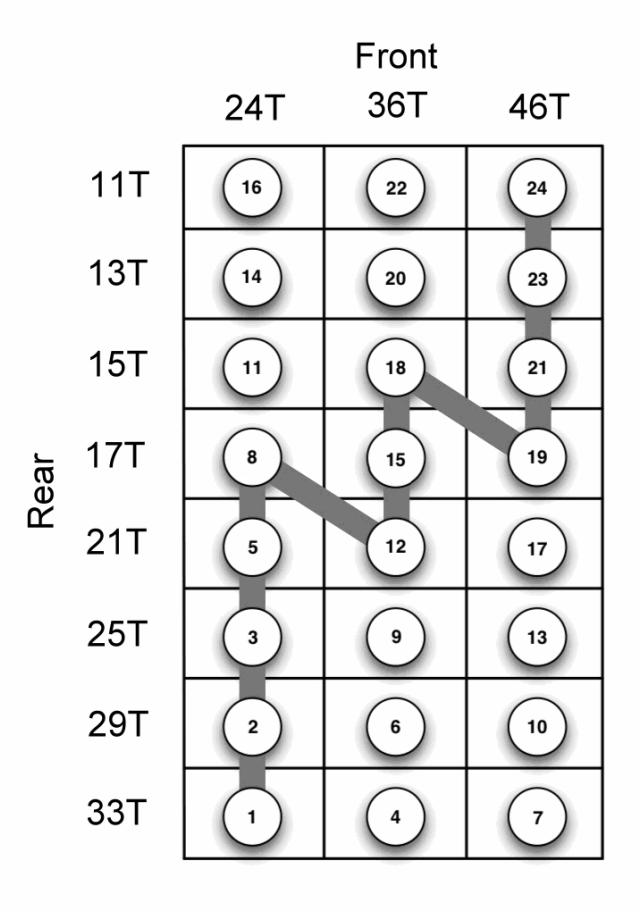

Fig 5.4 Fast gear-shifting sequence

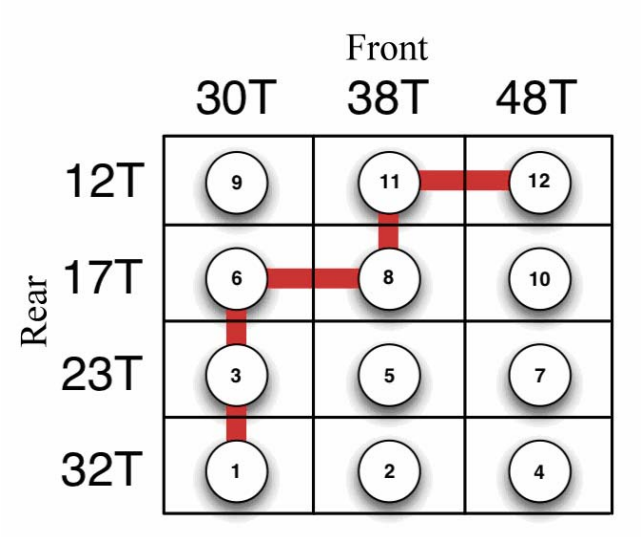

Fig 5.5 Gear-shifting sequence for Browning's system

Taking this result as the gear-shifting sequence will make the shifting strategy more comprehensive. After getting a new gear-ratio from the fuzzy logic controller, compare it to the mentioned 6 gear ratios of the sequence in Fig 5.8 and get a smaller and nearest one. For example, if the computed gear-ratio is rank 6 and the current is rank 11, then it needs one down-shifting on the gear, and one down-shifting on the rear gear. The procedure of the fully shifting strategy can be summarized as the follows:

1. When riders start riding, change the gear-ratio to the smallest one.
2. Acquire the velocity and the pedaling cadence information as shown in Fig 5.6 and 5.7.
3. Compute a new gear-ratio by fuzzy logic controller as shown in Fig 5.8.
4. Compare the new gear ratio to the current one. If two gear rations are equal, return to step 1.
5. Get the rank of the new gear-ratio from the sequence as shown in Fig 5.9.
6. Compute the shift times on front and rear derailleur systems as shown in Fig 5.9.
7. Send the commands to the derailleur systems and return to step 1.

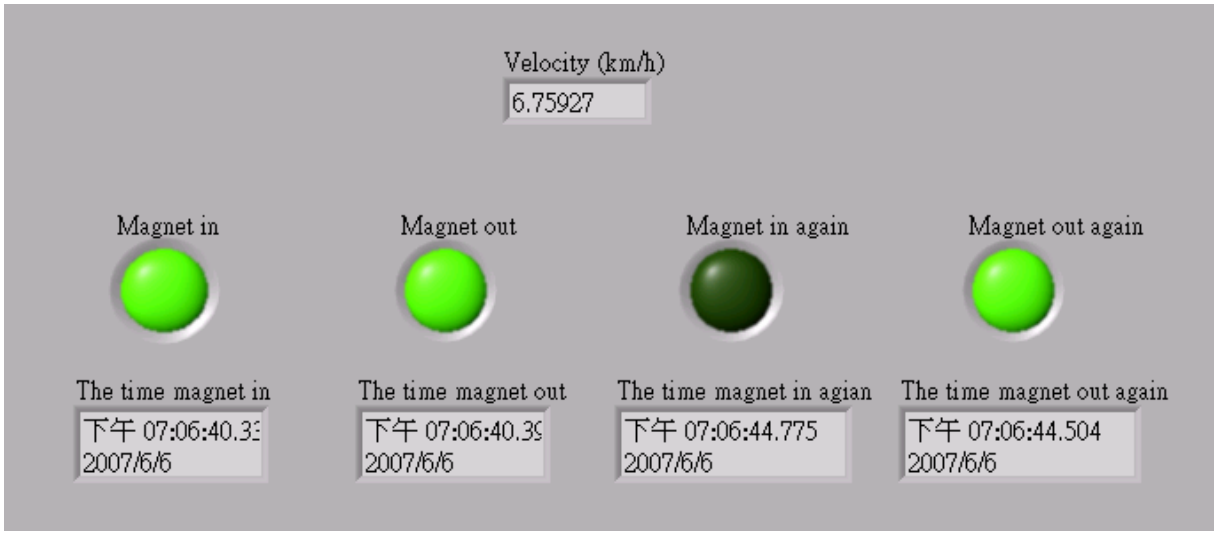

Fig 5.6 Compute the velocity by LabVIEW

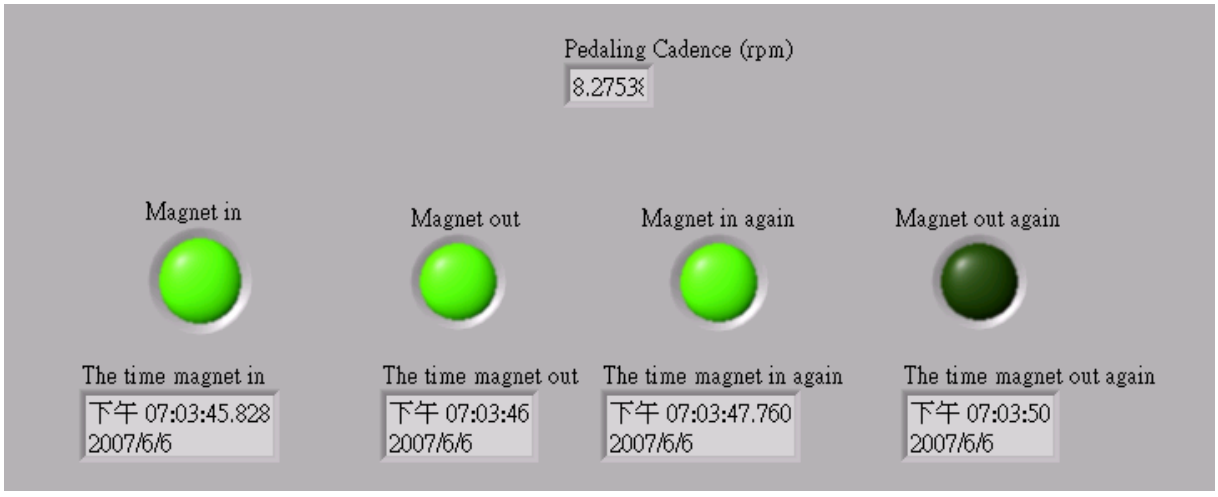

Fig 5.7 Compute the pedaling cadence by LabVIEW

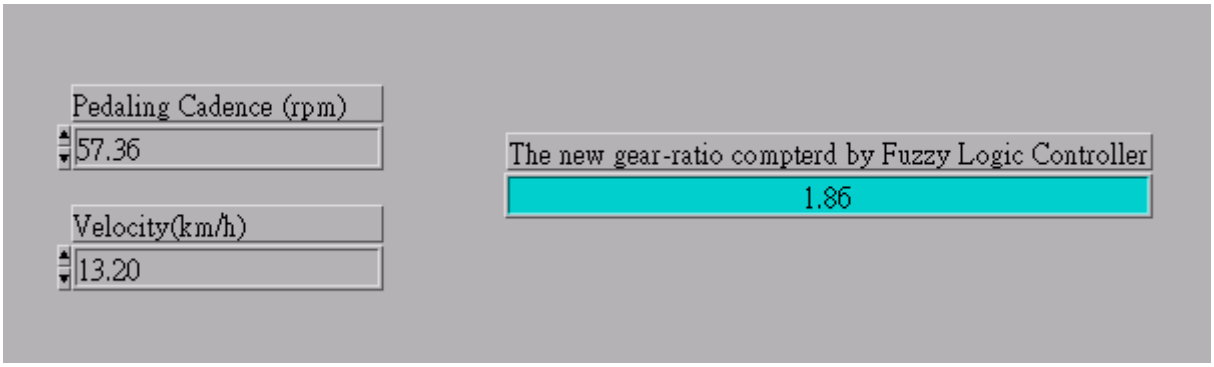

Fig 5.8 Computee the gear ratio using fuzzy logic controller by LabVIEW

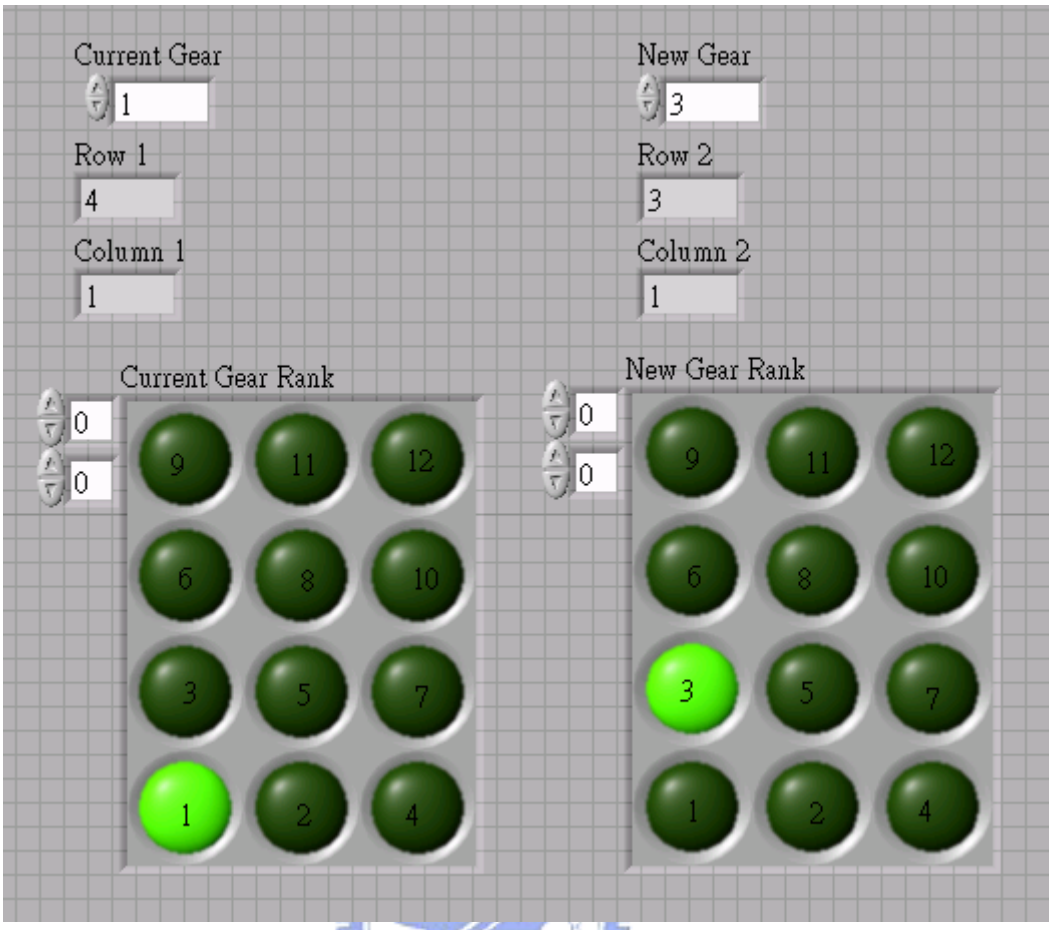

Fig 5.9 Get the rank and computing the shift times by LabVIEW

5.3.2 System Integration and Test

The signals from the magnetic reed switch are sent to the computer through the Line Printer Terminal (LPT). Then, the programs compute the time interval between two signals and obtain the current velocity and pedaling cadence. After the computer computes a new gear-ratio, it will send the shifting commands to the ECU through the RS232 port. And the ECU will send commands to the selector to actuate the derailleur systems. The fully system is shown in Fig 5.10.

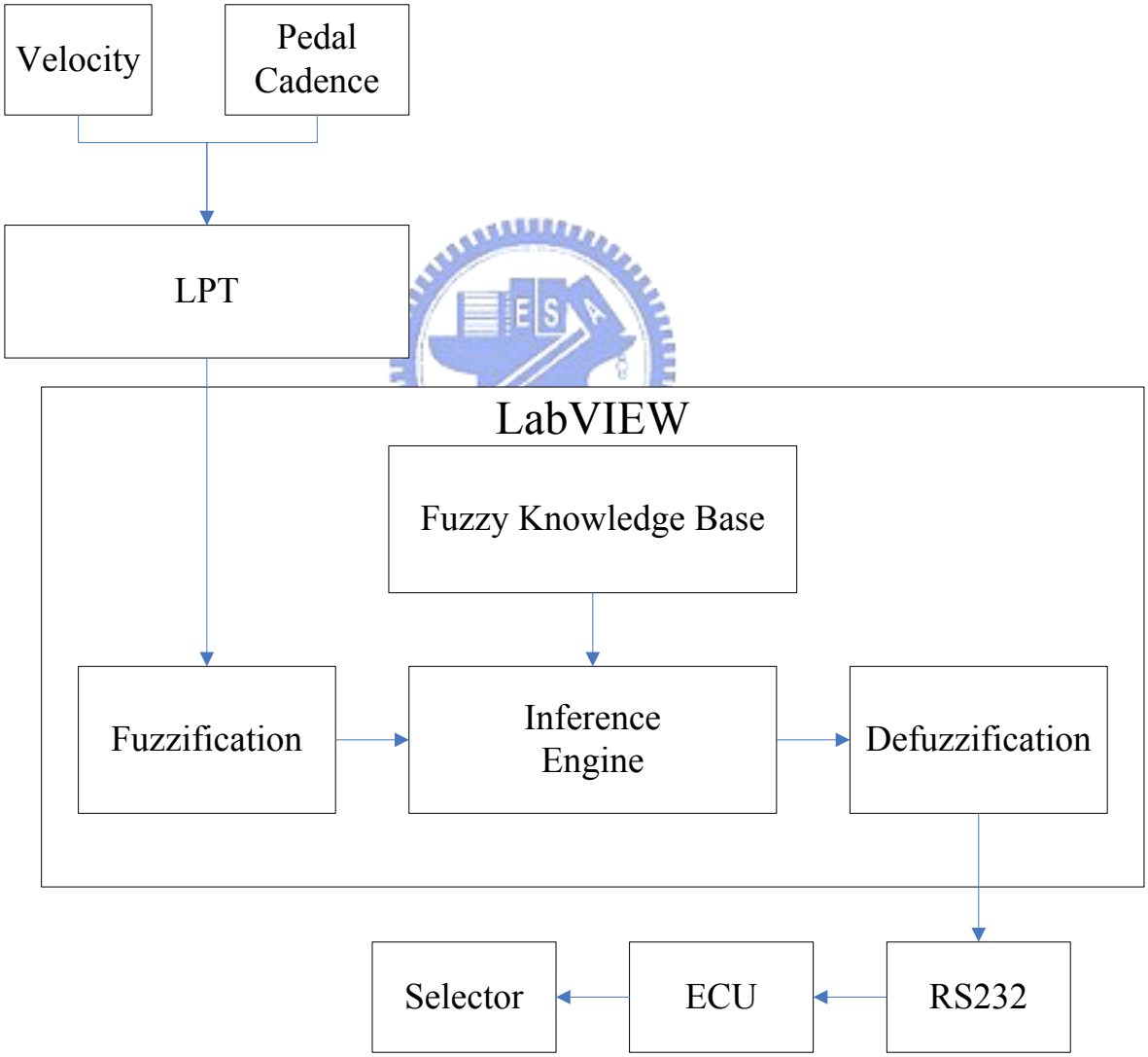

Fig 5.10 The Integrated System

After setting up the software and hardware, road tests can be performed to test the system. In order not to shift gears so frequently, the system get the velocity, pedaling cadence and output a gear-ratio every 5 seconds. The experimental data includes 200 data logs. It means that this experiment took about 16 minutes. As shown in Fig 5.11, between points 5 and 23, the velocity increases. It means that the rider is on a downgrade, so the gear-ratio is changed to a bigger one. On the other hand, the velocity and the pedaling cadence decrease between the points 23 and 27, it means that the rider is on an upgrade. Therefore, the gear-ratio is changed to a smaller one in order to make the rider feel more comfortable. Between points 1 and 5, the bicycle starts from the rest, so the gear-ratio is selected to a medium one in order to prevent the pedaling cadence excessively fast.

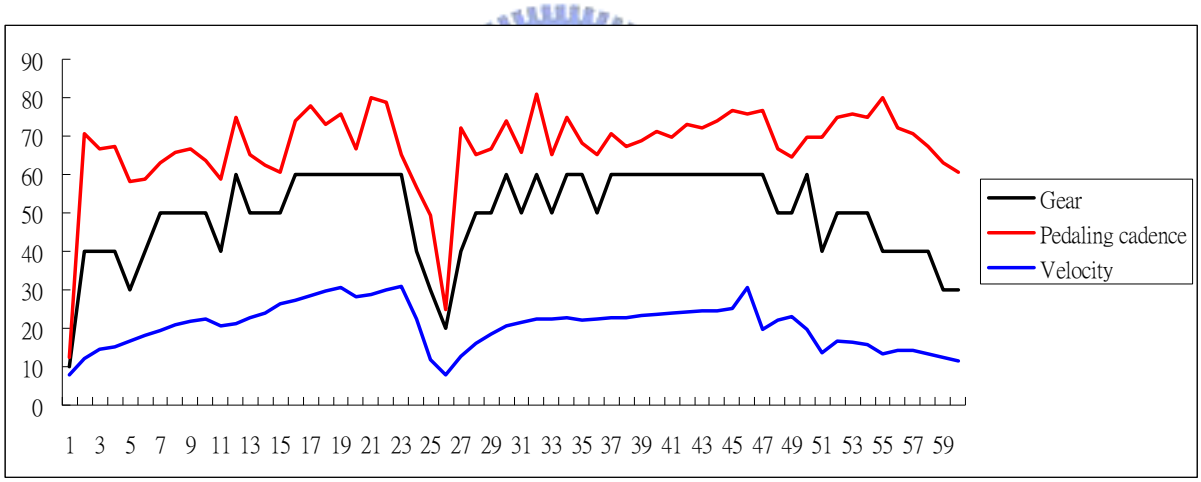

Fig 5.11 The system test results 1

There is another rider's test on the same route as shown in Fig 5.12. Between points 13 and 17, the velocity and the pedaling cadence increase. It means that the rider is on a downgrade; therefore the gear-ratio is selected to a big one. On the other hand, between the points 23 to 25, the velocity and the pedaling cadence decrease suddenly, it means that the rider is on an upgrade. For this reason, the gear-ratio is changed to a small one. And there is a similar appearance between the points 35 to 37.

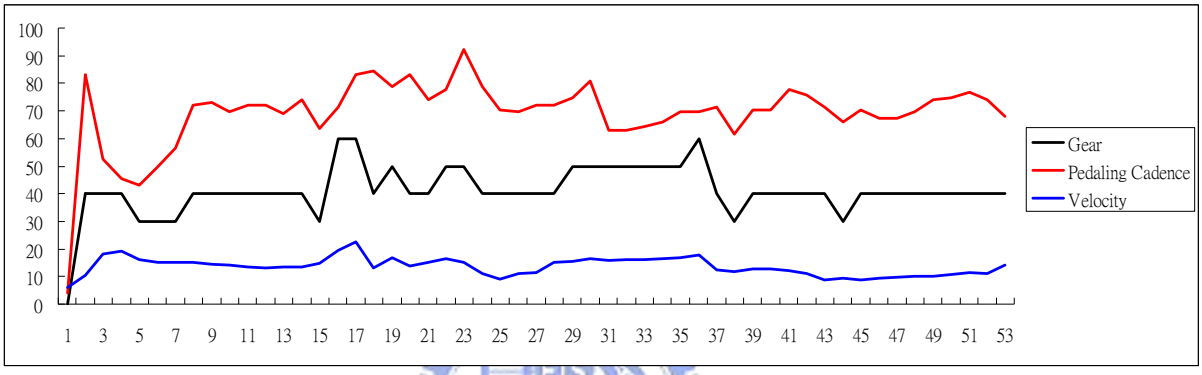

Fig 5.12 The system test results 2

There is another road test, shown in Fig 5.13. It tests on different route and by a different rider. Between the points 13 and 17, the velocity tends to decrease, but the pedaling cadence tends to increase, therefore the gear-ratio is changed to a big one to prevent the pedaling cadence excessively fast. And between the points 23 and 53, the velocity tends to increase; it means that the rider is on a downgrade condition, so the gear-ratio is also changed to a big one. Besides, between points 55 and 81, the velocity decreases slowly, it means the rider is on a gentle upgrade. For this reason, the gear-ratio is changed to a small one to make riding easy.

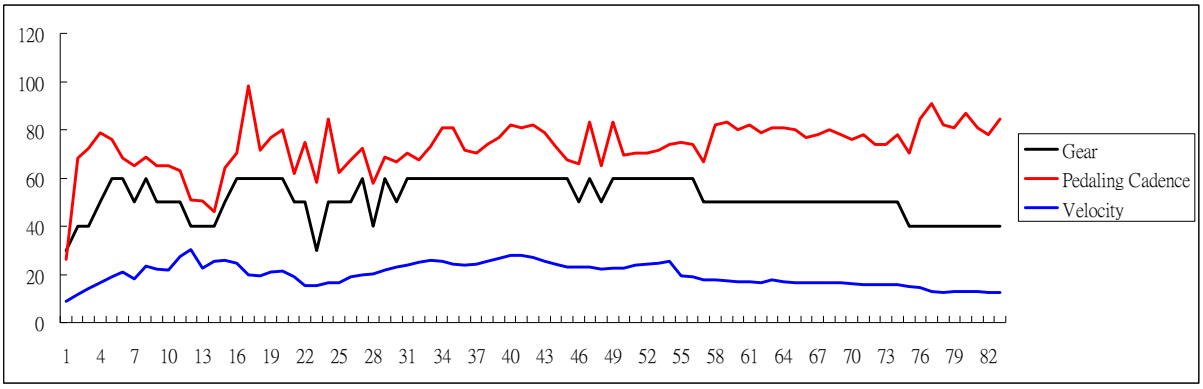

Fig 5.13 The system test results 3

There is still another test performance shown in Fig 5.14. It tests on the same route by another one rider as shown in Fig 5.12. Between points 1 to 10, the bicycle starts from the rest, both the pedaling cadence and the velocity increase, so the gear ratio is changed from a small one to a medium one and continued to change a big one. And between points 13 and 22, the pedaling cadence and the velocity tend to increase, it means that the rider is on a downgrade; hence the gear-ratio is changed to a big one. Between points 43 and 67, the velocity tends to decrease slowly; it is the same situation happened in the Fig 5.11. Therefore, the gear-ratio is also changed to a small one for the same reason.

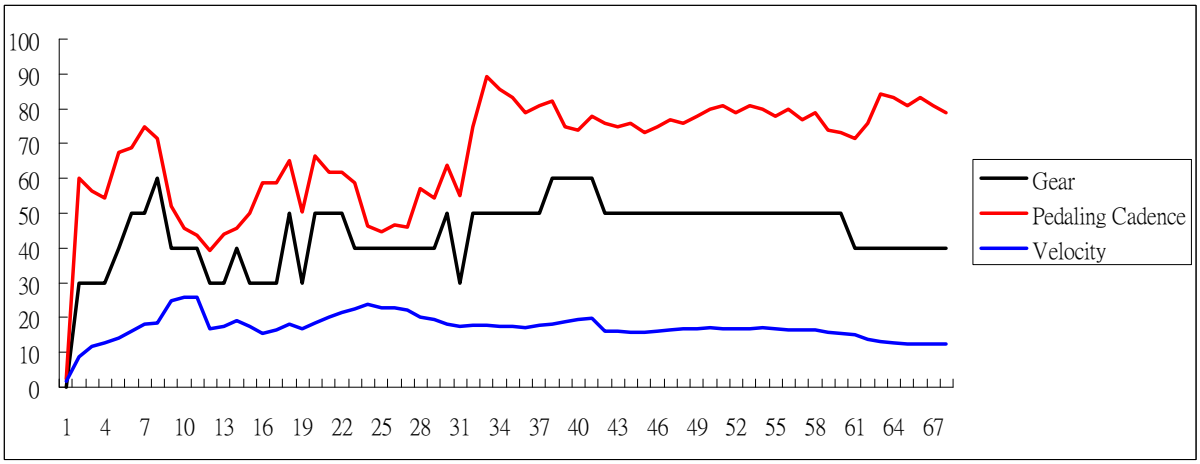

Fig 5.14 The system test results 4

By testing the original Browning SmartShift in the same way, the results are shown in Fig 5.14. Between points 1 and 23, the bicycle starts from the rest and rides on a downgrade. At the beginning, the velocity increases but the gear-ratio is not increase stable. When riders ride on a downgrade, although the trend of the gear ratio is increasing, the gear-ratio moves up and down in a short time. It makes riders feel uncomfortable and not easy to adjust pedaling cadence. Problem happens between points 25 and 47, the velocity decreases and the gear-ratio moves up and down in a short time. Besides, in points 11, 17, 31, and 36, the pedaling cadence are low but the gear-ratio are not changed to a small one, it make rider feel tiring and could not ride for a long time.

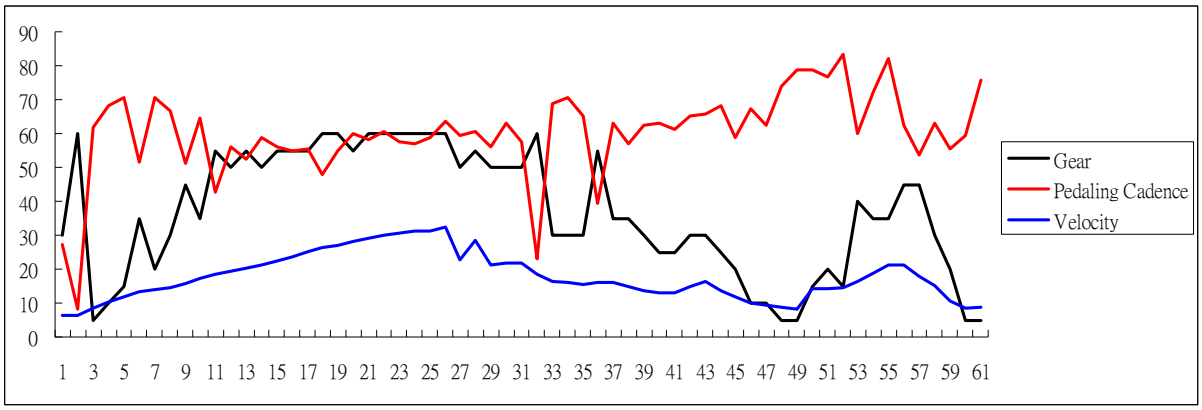

Fig 5.15 The Browning SmartShift sytem test result 1

There is another Browning SmartShift system test, shown in Fig 5.16. It tests by the same rider testing result shown in Fig 5.13. Between points 28 and 34, the pedaling cadence is low, but the gear-ratio is high, it would make rider feel uncomfortable.

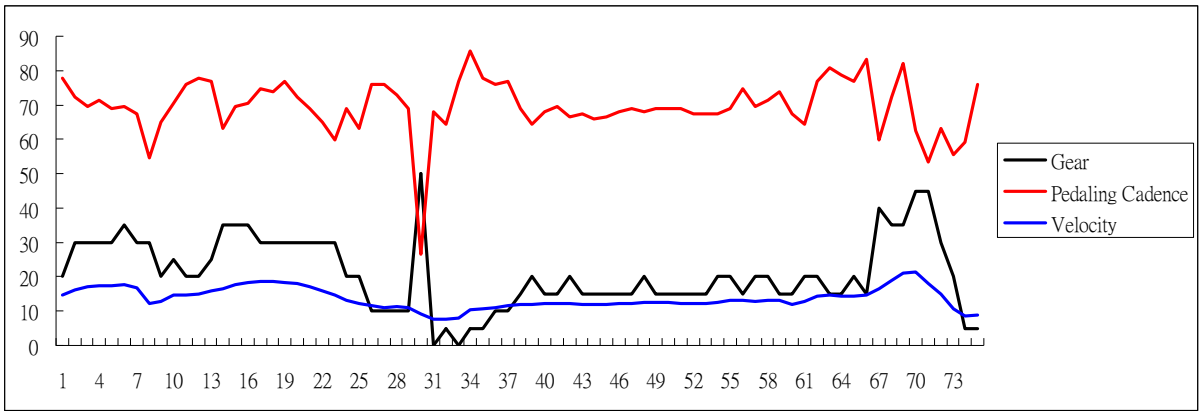

Fig 5.16 The Browning SmartShift sytem test result 2

The Browning SmartShift changes the gear ratio just depend on the velocity and ignores the pedaling cadence. But the pedaling cadence directly influences the rider's feeling. Besides, although the trends of the Browning Smartshift change gear-ratio usually matching the current situation, but the problem is: it changes too quickly and it makes rider not to maintain the pedaling cadence. That is the two obvious disadvantages of the Browning SmartShift.

The fuzzy logic controller changes gears depending on the velocity and the pedaling cadence. The results show that it can change gears not only matching the physical environments but also taking care of the riders. Therefore, it changes gears more stable and correct. And it changes not so frequently that can make riders easy to operate the bicycle and feel more comfortable. The pedaling cadence range of the four different riders is from 60 to 85 rpm, and these results match to the assumptions in the Chapter 3.

Based on the above statement, it is obvious that the fuzzy logic controller works well to improve the gear-shifting performance during riding bicycles.

CHAPTER 6

CONCLUSIONS AND FUTURE WORKS

6.1 Conclusions

There are many factors influencing the riders' performances. But the point is that if the riders know how to choose the gear-ratio and ride at the optimal cadence, then he or she can get the best performances or most comfortable feelings. In this study, the new shifting strategy is completed by fuzzy logic control theory. And it is implement using LabVIEW, and Browning SmartShift. It can test and get experiment data after combining the software and hardware. The conclusions of this study can be summarized as follows:

1. Choosing the optimal pedaling cadence range between 65 to 90 rpm can satisfy the all factors influencing the cycling performance in the prior researches.
2. Designing a fuzzy logic controller by designing the membership functions, constructing the if-then rule base, choosing the inference method and the defuzzification method. The new controller can decide how to change the gear-ratio and it is a new basic shifting strategy.
3. Integrating the fuzzy logic controller with the optimal gear-shifting sequence make the strategy more complete. The optimal gear-shifting sequence can decrease power lose during gear-shifting.
4. Combining the software(LabVIEW) and hardware(Browning SmartShift), the new gear-shifting strategy can perform road tests and get the experiment data.
5. Comparing the experiment results, the new shifting strategy performances is better than the Browning SmartShift system and the pedaling cadence ranges match the optimal cadence range chosen from the prior researches.

6.2 Further works

Although the control algorithms are developed and tested, there are still some further works should be accomplished in the future:

1. Improve the gear-shifting mechanism:

In this study, Browning SmartShift system was used to implement the algorithm. It is better to have a new gear-shifting mechanism in order that the algorithm can work efficiently.

2. Add the learning functions:

The fuzzy logic controller can fit different riders' needs by adjusting the membership functions and *if-then* rules. But it can not learn to adjust the algorithm according to different users. The learning functions can make the adjusting easier.

3. Develope more operation models:

For different riding conditions, the fuzzy membership functions and rule bases have to be adjusted. It can combine with the learning functions to adjust dynamically, or set different riding conditions, such as city riding, racing, or cross-country riding, in the bicycle computer.

REFERANCES

[1] 林聰穎，「自行車變速系統測試之研究」，國立交通大學，博士論文，民國 88 年。

[2] Redfield, R. and Hull, M. L., "On the relation between joint moments and pedaling rates at constant power in bicycling," Journal of Biomechanics, Vol. 19, No. 4, pp. 317-329, 1986.

[3] Redfield, R. and Hull, M. L., "Prediction of pedal forces in bicycling using optimization methods," Journal of Biomechanics, Vol. 19, No 7, pp. 523-540, 1986.

[4] Hull, M. L., Gonzalez, H. K. and Rob Redfield, "Optimization of pedaling rate in cycling using a muscle stress-based objective function," International Journal of Sport Biomechanics, Vol. 9, pp. 1-20, 1988.

[5] Marsh, A.P., Martin, P.E., and Sanderson, D. J., "Is a joint moment-based cost function associated with preferred cycling cadence," Journal of Biomechanics, Vol. 33, pp. 173-180, 2000.

[6] Neptune, R. R. and Hull, M. L., "A theoretical analysis of preferred pedaling rate selection in endurance cycling," Journal of Biomechanics, Vol. 32, pp. 409-415, 1999.

[7] Wilson, D. G., Bicycling Science, 3rd, MIT Press, Cambridge, MA, 2004.

[8] Marsh, A.P. and Martin, P.E., "The association between cycling experience and preferred and most economical cadences," Medicine and Science in Sports and Exercise, Vol. 25, No. 11, pp.1269-1274, 1993.

[9] Clark, R.K., Anatomy and Physiology, Jones and Bartlett Publishers, Sudbury, MA, 2005.

[10] Kent, M., Van De Graaff and Rhees, R. W., Human anatomy and physiologybased on Schaum's outline of theory and problems of human anatomy and physiology, McGraw-Hill, New York, 2001.

[11] Schneck, D. J. and Bronzino, J.D., Biomechanics—principles and applications, CRC

Press, Boca Raton, FL, 2003.

[12] Hull, M. L. and Jorge, M., “A method for biomechanical analysis of bicycle pedaling,” Journal of Biomechanics, Vol. 18, No. 9, pp.631-644, 1985.

[13] Neptune, R. R. and Herzog, W., “The association between negative muscle work and pedaling rate,” Journal of Biomechanics, Vol. 32, 1999.

[14] Woolford, S. M., Withers, R. T., Craig, N.P., Bourdon, P. C., Stanef, T. and Mckenzie, I., “Effect of pedal cadence on the accumulated oxygen deficit, maximal aerobic power and blood lactate transition thresholds of high-performance junior endurance cyclists,” European Journal of Applied Physiology, Vol. 80, pp. 285-291, 1999.

[15] Hagberg, J. M., Mullin, J. P., Giese, M. D. And Spitznagel, E., “Effect of pedaling rate on submaximal exercise responses of competitive cyclists,“ Journal of Applied Physiology, Vol. 51, pp. 447-451, 1981.

[16] Whitt, F. R. and Wilson, D. G., Bicycling Science, MIT Press, Cambridge, MA, 1982.

[17] Martin, J. C., Wagner, M. B. and Coyle, E. F., “Inertial-load method determines maximal cycling power in a single exercise bout,” Medicine and Science in Sports and Exercise, Vol. 29, No. 11, pp. 1505-1512, 1997.

[18] Zadeh, L., “Fuzzy sets,” Inf. Control, Vol.8, pp. 338-353, 1965.

[19] Leonid Reznik, Fuzzy Controllers, 1st, Victoria University of Technology, Melbourne, Australia, 1997.

[20] 陳曜丞，「智慧型控制介面於軍用腳踏車應用之研究」，國立國防大學，碩士論文，民國 94 年。